

# Inferring Causal Effects Under Heterogeneous Peer Influence

Shishir Adhikari, Elena Zheleva

University of Illinois Chicago, Chicago, IL, USA  
sadhik9@uic.edu, ezheleva@uic.edu

## Abstract

Causal inference in networks should account for interference, which occurs when a unit’s outcome is influenced by treatments or outcomes of peers. *Heterogeneous peer influence* (HPI) occurs when a unit’s outcome is influenced differently by different peers based on their attributes and relationships, or when each unit has a different susceptibility to peer influence. Existing solutions to estimating direct causal effects under interference consider either homogeneous influence from peers or specific heterogeneous influence mechanisms (e.g., based on local neighborhood structure). This paper presents a methodology for estimating individual direct causal effects in the presence of HPI where the mechanism of influence is not known a priori. We propose a structural causal model for networks that can capture different possible assumptions about network structure, interference conditions, and causal dependence and enables reasoning about identifiability in the presence of HPI. We find potential heterogeneous contexts using the causal model and propose a novel graph neural network-based estimator to estimate individual direct causal effects. We show that state-of-the-art methods for individual direct effect estimation produce biased results in the presence of HPI, and that our proposed estimator is robust.

## 1 Introduction

Causal inference is pivotal in making informed decisions across various domains, such as vaccination distribution (Barkley et al. 2020), policy making (Patacchini, Rainone, and Zenou 2017), and online advertising (Nabi et al. 2022). Causal inference involves modeling causal relationships and measuring the impact of interventions (or treatments) which aids in understanding policy effectiveness and designing targeted interventions. When units can impact each other’s outcomes, it is necessary to model this outcome *interference* explicitly and account for it in causal effect estimation. Research on causal inference with interference has a long history (Leavitt 1951; Halloran and Struchiner 1995) and has recently started to rely on graphical models (Maier et al. 2010; Maier 2014; Ogburn and VanderWeele 2014). Its focus is on estimating *direct effects* induced by a unit’s own treatment, *peer (or indirect) effects* induced by the treatments of other units, and *total effects* induced by both unit’s and others’ treatments (Hudgens and Halloran 2008).

Network experiment designs (Aral 2016; Ugander et al. 2013; Toulis and Kao 2013) and causal inference from observational network data (Arbour, Garant, and Jensen 2016;

Forastiere, Airoidi, and Mealli 2021; Jiang and Sun 2022) define *exposure mapping* (Aronow and Samii 2017) to control exposure to peer treatments for estimating direct, peer, or total effects. Most methods assume homogeneous (or equal) peer influence and use exposure mapping like the fraction of treated peers. However, *heterogeneous peer influence* (HPI) can occur when the influence of each peer on a unit varies based on the unit’s and peer traits, relationship characteristics, and network properties. Recent methods address HPI and focus on specific contexts such as local neighborhood structure (Yuan, Altenburger, and Kooti 2021), known node attributes (e.g., roles like parent-child or siblings) (Qu et al. 2021), known edge weights (Forastiere, Airoidi, and Mealli 2021) and group interactions (Ma et al. 2022). Our work focuses on estimating individual direct effects (IDE) where the HPI contexts and heterogeneous susceptibilities to peer influence are not known a priori.

As a motivating example, consider a toy social network, depicted in Figure 1, abstracted by a *schema* with entity class *User*, relationship class *Friend*, and attributes associated with each class. The instantiation of the schema is an attributed network capturing the existence and duration of friendship for users with different demographics, political affiliations, and stances on a policy issue (e.g., vaccination). The stances of individuals interacting in the social network can be influenced by their political affiliation and the affiliations and/or stances of their peers. Understanding the causal impact of an individual’s affiliation (the treatment) on the individual’s own stance (the outcome) requires individual direct effect (IDE) estimation while accounting for indirect effects from peer treatments. To illustrate heterogeneous peer influence, let us consider the ego networks for two units, depicted in Figure 2, where the units have the same number of treated and untreated friends but different network structures and peer attributes. Methods assuming homogeneous peer influence would produce the same representation of peer exposure (e.g., 33% treated) for the two units. However, peer exposure should be able to capture collective influence due to node attributes (e.g., similarity of age), edge attributes (e.g., closeness), and network structure (e.g., peer degree). For example, treated peers are mutual friends for unit A, and they may influence more collectively. A misspecified peer exposure may not control the indirect effects resulting in a biased IDE estimate. Similarly, peer exposure may be an effect modifier, i.e., a context that leads to heterogeneous IDE, and its misspecification biases the IDE estimates.

Under unknown HPI mechanisms, exposure mapping

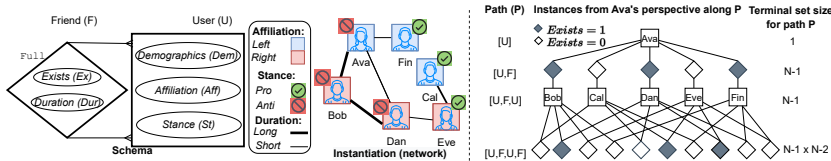


Figure 1: Schema, instantiation, and relational paths (i.e., traversal in the schema) for a toy social network. The paths capture an ego (e.g., Ava), the ego’s relationships, other nodes, and their relationships (except with the ego).

should be expressive to automatically capture relevant contexts but be invariant to irrelevant contexts. Moreover, accounting for confounders and effect modification contexts is crucial for any causal effect estimation task. Our work uses graphical causal modeling of interacting units to find such heterogeneous contexts. We propose a flexible and expressive *Network Structural Causal Model (NSCM)* that encodes assumptions about interference conditions, network structure, and causal dependencies. NSCM extends the relational causal model (RCM) (Maier 2014; Lee 2018) to incorporate relationship existence in networks (e.g., due to homophily), latent variables, and selection bias. Like RCM, it is able to handle arbitrary network models. Moreover, the *Network Abstract Ground Graph (NAGG)*, derived from NSCM, enables reasoning about the identification of heterogeneous treatment effects similar to the structural causal model (SCM) (Pearl 2009). We prove that NAGG is sound and complete for reasoning about relational d-separation. Using NSCM and NAGG, we can identify an adjustment set of relational variables to estimate individual direct effects (IDE). We propose a novel graph neural network-based estimator to estimate IDE by controlling potential confounders, heterogeneous peer influence contexts, and effect modifiers. We empirically show the robustness of our approach for the estimation of average and individual direct effects.

## 2 Related Work

Heterogeneous treatment effect estimation often assumes no interference and has focused on discovering heterogeneous contexts and estimating individual treatment effects (ITE) from i.i.d. data (Athey and Imbens 2016; Künzel et al. 2019; Qidong et al. 2020) and even from network data but without interference (Guo, Li, and Liu 2020; Gilad et al. 2021). ITE estimation (Johansson, Shalit, and Sontag 2016; Shalit, Johansson, and Sontag 2017) involves representation learning with neural networks to balance covariates in the treatment and control groups and predict counterfactual outcomes. We focus on causal modeling to facilitate representation learning for ITE estimation in networks with interference and we use graph neural networks (GNNs) (Kipf and Welling 2016; Xu et al. 2018) for representation learning.

There are two main lines of work on modeling causal inference with interference. The first one relies on the potential outcomes framework (Rubin 1974) and typically assumes that the variables that satisfy the unconfoundedness assumption (Rubin 1980) are known a priori (Hudgens and Halloran 2008; Forastiere, Airolidi, and Mealli 2021; Qu et al. 2021; Bargagli-Stoffi, Tortù, and Forastiere 2020). The second one relies on graphical models (Pearl 2009) which allow for the modeling of causal assumptions and reasoning about causal effect identification without requiring a priori knowledge about which variables would meet the uncon-

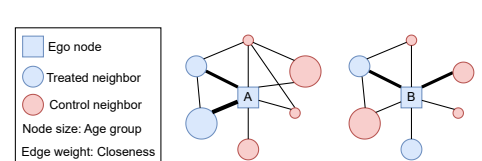


Figure 2: Two ego networks with the same number of treated and untreated friends but possibly different peer exposure conditions.

foundedness assumption. These works include causal diagrams for interference (Ogburn and VanderWeele 2014; Ogburn et al. 2022), chain graphs (Shpitser, Tchetgen, and Andrews 2017; Ogburn, Shpitser, and Lee 2020), structural causal models (SCMs) at the unit level with linear structural equations (Zhang, Mohan, and Pearl 2022), declarative languages (Salimi et al. 2020), and relational causal models (RCMs) (Arbour, Garant, and Jensen 2016; Maier 2014; Lee 2018). Multiple works have considered identifiability and estimation under specific SCMs with interference (Shalizi and Thomas 2011; Cristali and Veitch 2022; Fatemi and Zheleva 2023; Hayes, Fredrickson, and Levin 2022). Our causal modeling builds on RCMs because of their flexibility to represent and reason about causal dependence in relational domains and because they lend themselves to learning causal models from data (Maier et al. 2013; Lee and Honavar 2020). Here, we extend RCM to model mechanisms for relationship existence, such as homophily, as well as incorporate background knowledge of latent confounding, latent contexts, and selection bias whose implications have not been considered in previous work. While existing methods prefer certain network models (e.g., distinct clusters (McNealis, Moodie, and Dean 2023)) or mechanisms (e.g., equilibrium (Ogburn, Shpitser, and Lee 2020)), our model does not assume any specific network model, and by design, like RCM, is general for any network instantiation.

Most methods for estimating individual or heterogeneous causal effects under interference (Bargagli-Stoffi, Tortù, and Forastiere 2020; Jiang and Sun 2022; Ma and Tresp 2021; Ogburn et al. 2022) assume homogeneous interference between units. Recent works solving a diverse set of problems have partially addressed heterogeneous peer influence (HPI) due to known contexts (Qu et al. 2021; Forastiere, Airolidi, and Mealli 2021) or specific contexts (Yuan, Altenburger, and Kooti 2021; Ma et al. 2022; Tran and Zheleva 2022). Tran and Zheleva (2022) study peer contagion effects with homogeneous influence but different unit-level susceptibilities to the influence. Yuan, Altenburger, and Kooti (2021) capture peer exposure with causal network motifs, i.e., recurrent subgraphs in a unit’s ego network with treatment assignments. Ma et al. (2022) focus on addressing heterogeneous influence due to group interactions utilizing hypergraphs. We focus on causal modeling in networks that helps to identify relational random variables that capture unknown HPI contexts, confounders, and effect modifiers.

## 3 Causal Inference Problem Setup

We represent the network as an undirected graph  $G = (\mathcal{V}, \mathcal{E})$  with a set of  $N = |\mathcal{V}|$  vertices and a set of edges  $\mathcal{E}$ . We assume all vertices  $\mathcal{V}$  belong to a single entity class  $E$  (e.g., User) and the edges  $\mathcal{E}$  belong to a single relationship class  $R$  (e.g., Friend). We denote node attributes with  $\mathcal{A}(E)$  and edge attributes with  $\mathcal{A}(R)$ . Let  $X = \langle X_1, \dots, X_i, \dots, X_N \rangle$  be

a random variable comprising the treatment variables  $X_i$  for each node  $v_i$  in the network and  $Y_i$  be a random variable for  $v_i$ 's outcome. Let  $\pi = \langle \pi_1, \dots, \pi_i, \dots, \pi_N \rangle$  be an assignment to  $X$  with  $\pi_i \in \{0, 1\}$  assigned to  $X_i$ . Let  $X_{-i} = X \setminus X_i$  and  $\pi_{-i} = \pi \setminus \pi_i$  denote random variable and its value for treatment assignment to other units except  $v_i$ . We focus on estimating individual direct effects when the contexts for heterogeneous peer influence (HPI) and effect modification are not known a priori. Let  $\mathcal{Z}_i$  denote such unknown heterogeneous contexts that will be identified, in §4, as functions of node attributes, edge attributes, and network structure.

The *individual direct effect* (IDE) for a unit  $v_i$ , denoted as  $\tau_i$  or  $IDE(X_i = 1, X_{-i} = \pi_{-i}, \mathcal{Z}_i)$ , with treatment  $X_i = 1$  vs.  $X_i = 0$  given observed or assigned treatments of other units  $X_{-i} = \pi_{-i}$  and contexts  $\mathcal{Z}_i$  is defined as

$$\tau_i = E[Y_i(X_i = 1, X_{-i} = \pi_{-i}) | X_{-i} = \pi_{-i}, \mathcal{Z}_i] - E[Y_i(X_i = 0, X_{-i} = \pi_{-i}) | X_{-i} = \pi_{-i}, \mathcal{Z}_i], \quad (1)$$

where the counterfactual outcome of unit  $v_i$ ,  $Y_i(X_i = 1, X_{-i} = \pi_{-i})$ , expresses the idea that the outcome is influenced by the entire treatment assignment vector  $\pi$  due to interference. Equation 1 captures that peer exposure and other effect modifiers are defined by some function of treatments of other units  $X_{-i}$  and contexts  $\mathcal{Z}_i$ . Equation 1 is similar to Hudgens and Halloran (2008)'s Individual Direct Causal Effect estimand with fixed neighborhood treatment assignments. Using the consistency assumption (Pearl 2009, 2010) in causal inference that renders outcome generation independent of treatment assignment mechanisms (i.e., natural vs. intervention vs. counterfactual), we rewrite  $\tau_i$  as

$$\tau_i = E[Y_i(X_i = 1) | X_{-i} = \pi_{-i}, \mathcal{Z}_i] - E[Y_i(X_i = 0) | X_{-i} = \pi_{-i}, \mathcal{Z}_i]. \quad (2)$$

Equation 2, similar to Ma et al. (2022), differs from the "insulated" individual effects (Arbour, Garant, and Jensen 2016; Jiang and Sun 2022) that consider the effects with no peer exposure. In §4.4, we discuss the identifiability of individual effects  $\tau_i$  with experimental and observational data.

## 4 Causal Modeling and Reasoning

To model the data generation assumptions of a network  $G$ , including node attributes, the existence of edges, and edge attributes, we must define random variables for networks and link these variables to their causes, similar to the structural causal model (SCM). Building on the relational causal model (RCM), we propose Network Structural Causal Model (NSCM) and Network Abstract Ground Graph (NAGG), derived from the NSCM, for a more expressive representation of causal assumptions and reasoning identification of causal effects. We note that NSCM and NAGG are of independent interest beyond the scope of this paper for modeling causal assumptions in networks. Next, we introduce the concepts of relational schema, relational skeleton, and relational paths that are crucial to defining relational random variables. Then, we introduce encoding causal assumptions with relational dependencies between variables and reasoning identification of causal effects.

### 4.1 Modeling relationship existence

**Extended relational schema and skeleton.** We represent the network  $G(\mathcal{V}, \mathcal{E})$  as a single entity type and single relationship type (SESR) model (Maier 2014) with a schema  $S = (E, R, \mathcal{A})$  having entity class  $E$  (e.g., User), relationship class  $R = \langle E, E \rangle$  (e.g., Friend), node attributes

$\mathcal{A}(E)$ , and edge attributes  $\mathcal{A}(R)$ . We define relational skeleton, an instantiation of schema, to incorporate relationship existence uncertainty similar to DAPER (Heckerman, Meek, and Koller 2007) and PRM (Getoor et al. 2007) models.

**Definition 1** (Relational skeleton). A *relational skeleton*  $\sigma \in \Sigma_S$  for a schema  $S$  specifies sets of entity instances  $\sigma(E) = \mathcal{V}$  and relationship instances  $\sigma(R) = \Sigma_{\sigma(E)}$ , where  $\Sigma_{\sigma(E)}$  denotes relationship instance set with  $|\sigma(E)|$  fully-connected entity class instances and  $\Sigma_S$  denotes all possible skeletons.

**Definition 2** (Relationship existence indicator). A relationship existence indicator  $Exists \in \mathcal{A}(R) \wedge Exists \in \{0, 1\}$  is a relationship class attribute that is implicit, i.e., always present, and indicates the existence of an edge in  $G$ .

The above two definitions distinguish between relationship instances  $\sigma(R)$  and edges  $\mathcal{E}$ . As depicted in Figure 1, the relationship instances, indicated by diamond shapes, connect all nodes completely, but the *Exists* attribute indicates the presence of an edge. We allow attributes in the schema  $S = (E, R, \mathcal{A})$  to be marked as latent type or selection type. A *latent attribute set*  $L \in \mathcal{A}$  indicates the attributes that are always unmeasured. A *selection attribute set*  $S \in \mathcal{A}$  indicates conditioning on one or more attributes in  $\mathcal{A} \setminus S$ . Next, we will see the theoretical properties of these extended definitions using Maier (2014)'s notations and terminologies.

**Relational path and terminal set.** Random variables in networks should be defined from the perspective of entity/relationship (e.g., User), and their values can be multi-set. *Relational paths* and their *terminal sets* are building blocks for defining such variables. Figure 1 illustrates the relational paths and their terminal sets for base item *Ava* of class *User*. A *relational path*  $P = [I_j, \dots, I_k]$ , where  $I \in \{E, R\}$ , is an alternating sequence of entity and relationship classes. The path's beginning and ending item classes are called the base item class and terminal item class, respectively. A *terminal set*, denoted by  $P|_j^\sigma$ , relates a base item  $i_j \in \sigma(I_j)$  to a set of terminal items  $i_k \subseteq \sigma(I_k)$  according to *bridge burning semantics* (BBS) (Maier 2014) in a skeleton  $\sigma$ . As shown in Figure 1, BBS traverses  $\sigma$  along  $P$  in breadth-first order, beginning at  $i_j$ , to obtain terminal set  $P|_j^\sigma$  as tree leaves at level  $|P|$ . A relational path  $P$  is valid if its terminal set for any skeleton is non-empty, i.e.  $\exists \sigma \in \Sigma_S, \exists j \in \sigma(I), P|_j^\sigma \neq \emptyset$ .

**Lemma 1.** *In a SESR model, the terminal sets of any two relational paths under BBS, starting with a base item class  $I$ , do not intersect.*

**Proposition 1.** *A SESR model with relationship existence uncertainty has the maximum length of valid relationship paths  $[I_j, \dots, I_k]$  of four for  $I_j \in E$  and five for  $I_j \in R$  under bridge burning semantics (BBS) for any skeleton  $\sigma \in \Sigma_S$ .*

The proofs are presented in §A.5 and are based on Definitions 1 and 2 and BBS exploration. Lemma 1 allows us to rule out the complexity of intersecting paths (Maier 2014; Lee and Honavar 2015) in the SESR model. As illustrated in Figure 1, the entire network is represented from the perspective of users by the terminal sets of paths  $[E]$ ,  $[E, R]$ ,  $[E, R, E]$ , and  $[E, R, E, R]$  mapping to an ego, the ego's relationships, other nodes, and relationships between other nodes. This differs from RCM's SESR model (Arbour, Garant, and Jensen 2016), where relational paths can be infinitely long and capture entity or relationship instances at n-hops. In our case, we allow n-hop relations to change due to interventions or over time, and it is reflected in the *Exists* attribute of terminal sets of path  $[E, R]$  and  $[E, R, E, R]$ .

**Relational variable and relational dependency.** A *relational variable*  $P.X$  is composed of a relational path  $P$  and an attribute class  $X$ , where  $X$  is a terminal item class’s attribute. A relational variable is canonical if its relational path has a unit length. For our running example,  $[U].Aff$  is a canonical variable denoting the affiliation of users while  $[U, F].Ex$  denotes friendship existence. A *relational dependency*  $P.X \rightarrow [I].Y$ , where  $X \neq Y$ , is a pair of relational variables that share the same base item class  $I$ , and  $[I].Y$  is canonical. The use of canonical dependencies enables representation from the perspective of entity and relationship classes. For example, the dependency  $[F, U].Dem \rightarrow [F].Ex$  from the relationship class perspective captures the existence of an edge due to homophily where users with similar demographics tend to be friends. We model latent confounding and selection bias with dependencies of the form  $P.L_i \rightarrow [I].Y$  and  $P.X \rightarrow [I].S_i$ , respectively, where  $L_i \in \mathbf{L}$  and  $S_i \in \mathbf{S}$ . For example, the dependencies  $[F, U].L \rightarrow [F].Ex$  and  $[U].L \rightarrow [U].St$  jointly represent latent homophily and latent confounding. To represent contagion, we could introduce relational dependency with time-lagged attributes of the form  $[I].Y_L \rightarrow [I].Y$  and  $[I, \dots, I].Y_L \rightarrow [I].Y$ . The time-lagged attributes should mirror incoming and outgoing dependencies of  $Y$ , and these attributes could be unobserved i.e.,  $Y_L \in \mathbf{L}$ . We define *implicit dependencies* ( $\mathbf{D}_i$ ) to capture that the relationship attributes except *Exists*, i.e.,  $Exists' := \mathcal{A}(R) \setminus Exists$ , have non-default values only if the edge exists. For example, the duration of friendship is defined only if friendship exists.

**Definition 3** (Implicit dependencies). The *implicit relationship existence dependency set*  $\mathbf{D}_i$  is defined as  $\mathbf{D}_i := \{\forall Y \in Exists', [R].Exists \rightarrow [R].Y\}$ .

## 4.2 Network structural causal model (NSCM)

A *network structural causal model*  $\mathcal{M}(\mathcal{S}, \mathbf{D}, \mathbf{f})$  encapsulates a schema  $\mathcal{S}$ , a set of relational dependencies  $\mathbf{D}$ , and a set of functions  $\mathbf{f}$ . The functions relate each canonical variable  $[I].Y$  to its causes, i.e.,  $[I].Y = f_Y(pa([I].Y, \mathbf{D}), \epsilon_Y)$ , where  $f_Y \in \mathbf{f}$ ,  $pa([I].Y, \mathbf{D}) := \{P.X | P.X \rightarrow [I].Y \in \mathbf{D}\}$ , and  $\epsilon_Y$  is an exogenous noise. Generally, the functions  $\mathbf{f}$  in the model  $\mathcal{M}$  are unknown and estimated from the data. An NSCM to encode that a user’s and her friends’ affiliations affect the user’s stance needs three dependencies  $[U].Aff \rightarrow [U].St$ ,  $[U, F, U].Aff \rightarrow [U].St$ , and  $[U, F].Ex \rightarrow [U].St$ .

NSCM, like RCM, defines a template for how dependencies should be applied to data instantiations. A realization of NSCM  $\mathcal{M}$  with a relational skeleton  $\sigma$  is referred to as a ground graph  $GG_{\mathcal{M}\sigma}$  (Maier 2014) (definition in §A.5). It is a directed graph with vertices as attributes of entity instances (like  $Bob.Aff$  and  $Ava.St$ ) and relationship instances (like  $\langle Bob-Ava \rangle.Dur$ ), and edges as dependencies between them. An acyclic ground graph has the same semantics as a standard graphical model (Getoor et al. 2007), and it facilitates reasoning about the conditional independencies of attribute instances using standard d-separation (Pearl 1988). However, it is more desirable to reason about dependencies that generalize across all ground graphs by using expressive relational variables and abstract concepts. A higher-order representation known as an abstract ground graph (AGG) (Maier 2014; Lee 2018) has been developed for this purpose. Relational d-separation (Maier 2014) is the standard d-separation applied on AGG.

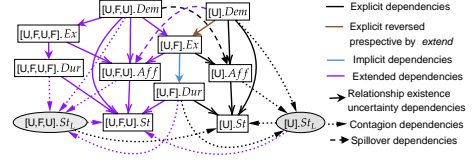


Figure 3: A network abstract ground graph (NAGG) for the toy social network capturing homophily, spillover, contagion, and potential sources of heterogeneity.

## 4.3 Network abstract ground graph (NAGG)

A network abstract ground graph ( $NAGG_{\mathcal{M}B}$ ), for the NSCM  $\mathcal{M}$  and a perspective  $B \in \mathbf{I}$ , is a representation to enable reasoning about relational d-separation consistent across all ground graphs using relational variables ( $RV$ ) and edges between them ( $RVE$ ). An  $RV$  is a set of all relational variables of the form  $[B, \dots, I_k].X$ , with  $|RV|$  dependent on  $B$  for the SESR model (Proposition 1). An  $RVE \subset RV \times RV$  is a set of edges between pairs of relational variable obtained after applying *extend* (Maier 2014) operator on relational dependencies, i.e.,  $RVE = \{[B, \dots, I_k].X \rightarrow [B, \dots, I_j].Y | [I_j, \dots, I_k].X \rightarrow [I_j].Y \in \mathbf{D}\}$ , where  $[B, \dots, I_k] \in extend([B, \dots, I_j], [I_j, \dots, I_k])$  and  $[B, \dots, I_k]$  is a valid path (Proposition 1). Figure 3 depicts a network abstract ground graph ( $NAGG_{\mathcal{M}B}$ ) from the perspective  $B = User$  entity class for an NSCM  $\mathcal{M}(\mathcal{S}, \mathbf{D})$  with the toy social network schema. The NSCM encodes the causal hypotheses with explicit relational dependencies  $\mathbf{D}$  indicated by black and brown edges. These dependencies capture: (1) the existence of friendship depends on demographics; (2) stance is affected by one’s affiliation; (3) one’s demographics confounds affiliation and stance while peer demographics influence one’s affiliation; and (4) a user’s stance is influenced by other users’ stance depending on friendship duration. All the explicit dependencies and the implicit dependency (see blue arrow) for relationship existence uncertainty, are extended (see purple arrows) to capture dependencies between all relational variables for a given perspective.

A relational model is acyclic if its *class dependency graph* with vertices as attribute classes and edges as dependencies between them is acyclic (Getoor et al. 2007). For simplicity of exposition, we will assume the NSCM model  $\mathcal{M}(\mathcal{S}, \mathbf{D})$  is acyclic. The relational d-separation queries can be answered by applying standard d-separation on  $NAGG_{\mathcal{M}B}$  with vertices  $RV$  and edges  $RVE$ . We extend the theoretical properties of AGG (Maier 2014) to NAGG with relationship existence uncertainty, latent attributes, and selection attributes. Let sets  $\mathbf{L}$  and  $\mathbf{S}$  also include latent and selection relational variables. The proofs, presented in §A.5, follow the Maier (2014)’s proof of soundness and completeness considering the implications of selection and latent variables.

**Theorem 1.** For every acyclic NSCM  $\mathcal{M}$  and perspective  $B \in \{E, R\}$ , the  $NAGG_{\mathcal{M}B}$  is sound and complete for all ground graphs  $GG_{\mathcal{M}\sigma}$  with  $\sigma \in \Sigma_{\mathcal{S}}$ .

**Corollary 1.** For every acyclic NSCM  $\mathcal{M}$  and perspective  $B \in \{E, R\}$ , the  $NAGG_{\mathcal{M}B}$  is directed and acyclic.

**Theorem 2.** Relational d-separation is sound and complete for NAGG. Let  $\mathcal{M}$  be an acyclic NSCM and let  $\mathbf{X}$ ,  $\mathbf{Y}$ , and  $\mathbf{Z} | \mathbf{L} \notin \mathbf{Z} \wedge \mathbf{L} \cup \mathbf{S} \in \mathcal{A}$  be three distinct sets of relational variables for perspective  $B \in \{E, R\}$  defined over schema  $\mathcal{S}$ . Then,  $\mathbf{X}$  and  $\mathbf{Y}$  are d-separated by  $\mathbf{Z}$  on the  $NAGG_{\mathcal{M}B}$  if

and only if for all skeletons  $\sigma \in \Sigma_S$  and for all  $b \in \sigma(B)$ ,  $\mathbf{X}|_b$  and  $\mathbf{Y}|_b$  are  $d$ -separated by  $\mathbf{Z}|_b$  in ground graph  $GG_{M\sigma}$ .

With these theoretical properties, NAGG enables reasoning about the identification of causal effects in networks using counterfactual reasoning with the SCM (Pearl 2009).

#### 4.4 Identification of causal effects

Given a NAGG (e.g., Figure 3) we can reason the identifiability of causal effects using do-calculus (e.g., backdoor adjustment) (Pearl 2009). Here, we discuss the identification of IDE in Equation 2 using NSCM and NAGG for a more general assumption in experimental and observational studies like A/B tests and prospective cohort studies.

**Assumption 1.** The network  $G$  and its attributes are measured before treatment assignments and treatments are immutable from assignment to outcome measurement.

For node attributes  $\mathbf{Z}_n$  and edge attributes  $\mathbf{Z}_e$ , we denote relational variables  $[E, \mathbf{Z}_n]$ ,  $[E, R, \mathbf{Z}_e]$ ,  $[E, R, E, \mathbf{Z}_n]$ , and  $[E, R, E, R, \mathbf{Z}_e]$  with the notations  $Z_i \in \mathbb{R}^d$ ,  $Z_r \in \mathbb{R}^{N' \times d'}$ ,  $Z_{-i} \in \mathbb{R}^{N' \times d}$ , and  $Z_{-r} \in \mathbb{R}^{N' \times N' - 1 \times d'}$ , respectively, where  $N' = |\mathcal{V}| - 1$  and  $< d, d' >$  are constants. Let  $E_r \in \{0, 1\}^{N' \times 1}$  and  $E_{-r} \in \{0, 1\}^{N' \times N' - 1 \times 1}$  be the relationship existence indicator variables  $[E, R].Exists$  and  $[E, R, E, R].Exists$ , respectively. Under Assumption 1, the underlying data generation of treatment and outcome can be described by functions  $f_X$  and  $f_Y$  in our general NSCM as:  $X_i = f_X(Z_i, Z_r, Z_{-i}, Z_{-r}, E_r, E_{-r}, X_i^L, X_{-i}^L, \epsilon_X)$  and  $Y_i = f_Y(X_i, X_{-i}, Z_i, Z_r, Z_{-i}, Z_{-r}, E_r, E_{-r}, Y_i^L, Y_{-i}^L, \epsilon_Y)$ , where  $\{X_i^L, X_{-i}^L, Y_i^L, Y_{-i}^L\}$  are latent time-lagged variables for treatment and outcome. The NSCM allows both latent homophily and contagious treatments or outcomes. Causal inference with observational data often relies on the *unconfoundedness condition* which is untestable.

**Lemma 2.** *If there exists any adjustment set  $\mathbf{W}$  that satisfies the unconfoundedness condition (Rubin 1980), i.e.,  $\{Y_i(X_i = 1), Y_i(X_i = 0)\} \perp\!\!\!\perp X_i | \mathbf{W}$ , then the adjustment set  $X_{-i} \cup \mathbf{Z}_i$ , where  $\mathbf{Z}_i = \{Z_i, Z_r, Z_{-i}, Z_{-r}, E_r, E_{-r}\}$  also satisfies the condition under Assumption 1.*

The proof, in §A.6, is based on the fact that  $X_{-i} \cup \mathbf{Z}_i$  is a valid maximal adjustment set for the NSCM above.

**Corollary 2.** *Under Assumption 1, the counterfactual term  $E[Y_i(X_i = \pi_i) | X_{-i}, \mathbf{Z}_i]$  can be estimated as  $E[Y_i | X_i = \pi_i, X_{-i}, \mathbf{Z}_i]$  from experimental data or from observational data if Lemma 2’s condition holds.*

The proof for Corollary 2, in §A.6, follows from do-calculus (Pearl 2009) applied to NAGG derived from NSCM for experimental (with randomized but correlated treatments) and observational data (with no unobserved confounders between  $X_i$  and  $Y_i$ ). §A.6 discusses the implications on the identifiability when the assumptions are violated. Next, we present our empirical estimation framework.

### 5 Empirical estimation

We present a framework (IDE-TARNet), depicted in Figure 4, for empirical estimation of individual direct effects (IDE) that consists of two key steps: (1) mapping raw inputs to feature representations, and (2) estimating IDE using *counterfactual outcome (CFO)* prediction. The CFO prediction estimand  $E[Y_i | X_i = \pi_i, X_{-i}, \mathbf{Z}_i]$  can be learned with supervised learning. However, the values of relational

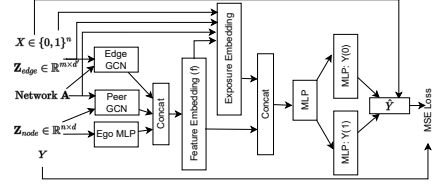


Figure 4: Proposed GNN-based estimator (IDE-TARNet).

variables in  $\{X_{-i} \cup \mathbf{Z}_i \setminus Z_i\}$  are multi-sets and should be summarized with appropriate functions. Moreover, the relational variables  $\phi(X_{-i}, \mathbf{Z}_i)$  should approximate the underlying heterogeneous peer influence (HPI) strength to control indirect effects. Similar to other state-of-the-art (SOTA) approaches (Arbour, Garant, and Jensen 2016; Jiang and Sun 2022; Yuan, Altenburger, and Kooti 2021), we assume interference occurs from neighbors to summarize values of relational variables and peer influence. Next, we describe feature and exposure embeddings to map the raw attributed network to relational variables and their interactions to capture potential confounders, effect modifiers, and HPI contexts.

**Feature mappings.** The inputs to the framework are adjacency matrix  $\mathbf{A}$  with  $n$  nodes and  $m/2$  undirected edges, treatment  $X \in \{0, 1\}^n$ , outcome  $Y \in \mathbb{R}^n$ , node attributes  $\mathbf{Z}_n \in \mathbb{R}^{n \times d}$  and edge attributes  $\mathbf{Z}_e \in \mathbb{R}^{m \times d'}$ . Ideally, a feature mapping should capture sufficient statistics about the underlying distribution of relational variables in  $\mathbf{Z}_i$  and their interactions. The feature mapping  $\phi_f$  maps network structure, node attributes, and edge attributes in  $\mathbf{Z}_i$  to an embedding vector of dimension  $l$ , i.e.,  $\phi_f(\mathbf{Z}_n, \mathbf{Z}_e, \mathbf{A}) \rightarrow \mathbb{R}^{n \times l}$ . We propose GNN feature embeddings  $h_f$  by concatenating outputs of ego multi-layer perception (MLP)  $h_i$ , the peer graph convolution network (GCN)  $h_{-i}$ , and edge GCN  $h_r$  modules capturing relational variables  $\phi_i(Z_i)$ ,  $\phi_{-i}(Z_{-i}, E_r)$ , and  $\phi_r(Z_r, Z_{-r}, E_r, E_{-r})$ , respectively. We defer the formal definitions of  $h_i$ ,  $h_{-i}$ , and  $h_r$  to Appendix A.3.

**Exposure mapping.** The exposure mapping  $\phi_e$  maps the treatment of other units, the feature embeddings, raw network, and edge attributes to an embedding vector of dimension  $k$ , i.e.,  $\phi_e(X, h_f, \mathbf{A}, \mathbf{Z}_e) \rightarrow \mathbb{R}^{n \times k}$ . Ideally, the exposure mapping under unknown HPI mechanisms should be expressive to capture relevant contexts but also invariant to irrelevant contexts. To maintain expressiveness, we consider exposure mapping as a weighted fraction of peers with multiple candidate weights based on edge attributes, peer features, similarity with peers, and network structure. We defer the formal definition to the Appendix A.3. The embedding  $h_e$  is passed to the downstream IDE estimator to strengthen invariance to irrelevant mechanisms for outcome prediction.

**Individual direct effect (IDE) estimation.** The feature and exposure embeddings, capturing representation for each node in the network, can be plugged into existing ITE estimators. For exposition and reproducibility, we demonstrate IDE estimation with the TARNet approach (Shalit, Johansson, and Sontag 2017) that uses CFO prediction agnostic of treatments, i.e.,  $\hat{Y}(1) = \Theta_1(h)$ ,  $\hat{Y}(0) = \Theta_0(h)$ , and  $\hat{Y} = \hat{Y}(1)$  if  $X = 1$  else  $\hat{Y}(0)$ , where  $\Theta$  is a MLP and  $h = \Theta(h_f || h_e)$ . We optimize the model to minimize the loss  $\mathcal{L} = (Y - \hat{Y})^2 + \lambda_{se}^{-\gamma \times \sigma_{\hat{Y}}^2} \sigma_{\hat{Y}}^2$ , where  $\hat{\tau} = Y(1) - Y(0)$  is estimated effect and  $\sigma_{\hat{Y}}^2$  is the variance. Here, the second term is a regularization to smooth variance in estimated causal ef-

fects controlled by scale parameter  $\lambda_s$  and decay parameter  $\gamma$ . Due to the decay term, the regularization gets stronger for smaller variances and weaker for larger variances smoothing the variance of estimated effects.

Here, the choice of embeddings and estimator in the framework is for illustrative purposes. The embeddings could use a different GNN (e.g., GAN (Veličković et al. 2018)) and the estimator with a different learner (e.g., X-learner (Künzel et al. 2019)). One of the reasons to choose this specific representation and estimator is based on the fact that recent works without HPI relied on them (Guo, Li, and Liu 2020; Jiang and Sun 2022), which helps with fair empirical comparison to the baselines. The choice of the estimator part of IDE-TARNet is driven by the fact that we needed an estimator that can handle network data. Some ITE estimators have been extended to work for network data, including causal trees (Bargagli-Stoffi, Tortù, and Forastiere 2020), inverse probability weighting (IPW) (Qu et al. 2021), and doubly-robust (McNealis, Moodie, and Dean 2023) but not all of them are suitable for observational data, unknown HPI contexts, or all network models.

## 6 Experiments

Here, we investigate the necessity of addressing HPI for robust IDE estimation. To establish robustness, we assess the performance of IDE estimators in various network settings with different topologies, edge densities, and causal data generation mechanisms. We evaluate errors in the estimation of constant and heterogeneous direct effects in the presence of HPI due to various mechanisms.

### 6.1 Experimental Setup

As it is common in causal inference tasks, we rely on synthetic and semi-synthetic datasets for evaluation because the ground truth causal effects and heterogeneity contexts are unknown in real-world data. We investigate the robustness of estimators for various network topologies and edge densities using synthetic data. For semi-synthetic data, we use real-world networks and attributes and generate the treatments and outcomes to evaluate estimators in more realistic and complex network settings.

**Synthetic data.** We consider two random network models: (1) the Barabási Albert (BA) model (Albert and Barabási 2002), which captures preferential attachment phenomena (e.g., social networks) with a few highly connected and others poorly connected nodes, and (2) the Watts Strogatz (WS) model (Watts and Strogatz 1998), which captures small-world phenomena characterized by high clustering and short path lengths between nodes. We generate both networks fixing  $N = 3000$  and controlling the sparsity of edges. The topology and sparsity of networks should be considered to evaluate robustness because, as shown in §6.2, they impact underlying peer influence and thus the estimation of IDE. For the BA model, sparsity is controlled by the preferential attachment parameter  $m$ , whereas sparsity in the WS model is controlled by the mean degree parameter  $k$  with a fixed rewiring probability of 0.5. We discuss the instantiation of treatment  $X$  and outcome  $Y$  and defer the generation of node attributes  $\{C, Z\} \subset \mathbf{Z}_n$ , consisting confounder and effect modifier, and edge attributes  $\{Z_r\} \subset \mathbf{Z}_e$  to §A.4.

**Treatment model.** For observational data, a unit’s treatment may be influenced by its own covariates and peer treatments or covariates. We generate treatment  $X_i$  as  $X_i \sim$

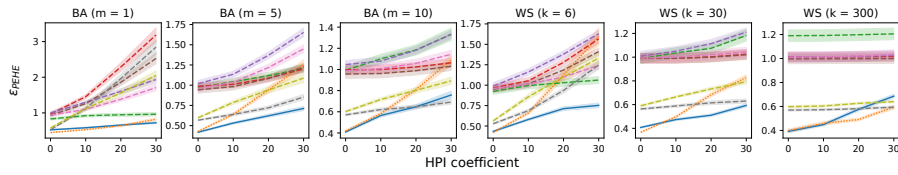
$\theta(a(\tau_c \mathbf{W}_x \cdot \frac{\sum E_r \odot C_{-i}}{\sum E_r} + (1 - \tau_c) \mathbf{W}_x \cdot C_i))$ , where  $\theta$  denotes Bernoulli distribution,  $a$  is an activation function,  $\tau_c \in [0, 1]$  controls influence from peers, and  $\mathbf{W}_x$  is the weight matrix.

**Outcome model.** We define the outcome  $Y_i$  as a function of unit’s treatment ( $\tau_d$ ), attribute effect modifier ( $\tau_a$ ), network effect modifier ( $\tau_n$ ), HPI contexts ( $\tau_p, \tau_{Z_r}, \tau_{Z_{-i}}, \tau_{E_{-r}}$ ), confounder ( $\tau_{c1}$ ), and random noise ( $\epsilon$ ). We defer the detailed functional form of the outcome model to the Appendix A.4. The coefficients  $\tau_a$  and  $\tau_n$  control treatment effect modification based on node attributes (e.g., age group) and network location (e.g., degree centrality), respectively. We model HPI based on the strength of ties ( $\tau_{Z_r}$ ), attribute similarity ( $\tau_{Z_{-i}}$ ), local structure captured by mutual friend count ( $\tau_{E_{-r}}$ ), and combination of them. Peer exposure coefficient ( $\tau_p$ ) controls the strength of HPI.

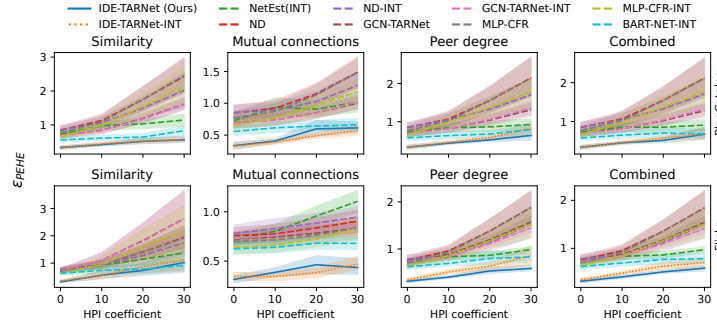
**Semi-synthetic data.** Following previous work (Guo, Li, and Liu 2020), we use two real-world social networks, Blog-Catalog and Flickr, with more realistic topology and attributes to generate treatments and outcomes. We use the LDA (Blei, Ng, and Jordan 2003) topic model to reduce the dimensionality of raw features to 50. The 50-dimensional features are randomly assigned to either confounding set  $\mathbf{C}$  or effect modifier set  $\mathbf{Z}$ . Both real-world networks lack edge attributes and we consider the HPI based on friends’ degrees instead of the strength of ties. The detailed functional forms for treatment and outcome models are included in §A.4.

**Evaluation metrics.** To evaluate the performance of heterogeneous effect estimation, we use the *Precision in the Estimation of Heterogeneous Effects* ( $\epsilon_{PEHE}$ ) (Jiang and Sun 2022; Ma and Tresp 2021) metric defined as  $\epsilon_{PEHE} = \sqrt{\frac{1}{n} \sum_i (\tau_i - \hat{\tau}_i)^2}$ , where  $\tau_i$  and  $\hat{\tau}_i = Y_i(1) - Y_i(0)$  are true and estimated IDEs.  $\epsilon_{PEHE}$  (lower better) measures the deviation of estimated IDEs from true IDEs. To evaluate the performance of average IDE estimation, we use  $\epsilon_{ATE}$  metric defined as  $\epsilon_{ATE} = |\frac{1}{N} \sum_{v_i \in \mathbf{V}} \tau_i - \frac{1}{N} \sum_{v_i \in \mathbf{V}} \hat{\tau}_i|$  that gives absolute deviation from true average IDEs.

**Estimators.** We compare our proposed estimator, IDE-TARNet, with NetEst (Jiang and Sun 2022), a recently proposed GNN-based state-of-the-art estimator that considers the fraction of treated peers as exposure embedding (INT). Additionally, we use IDE-TARNet-INT as a baseline that only utilizes feature embeddings and considers vanilla exposure embedding like NetEst. Following NetEst paper (Jiang and Sun 2022), we also include estimators MLP-CFR (Shalit, Johansson, and Sontag 2017), ND (or GCN-CFR) (Guo, Li, and Liu 2020), and GCN-TARNet with no-interference assumption and vanilla exposure embedding as baselines. For the semi-synthetic experiments, we include a baseline BART-NET-INT, based on BART (Hill 2011), a tree-based estimator, with mean peer covariates and homogeneous influence because it had a competitive performance on the datasets (Guo, Li, and Liu 2020) in §A.1. Figure 9 in the appendix, compares the performance of the causal network motifs approach (related work considering HPI due to local structure) with IDE-TARNet. Other works are not directly applicable as the baselines due to their scope (e.g., group interactions or contagion effects) or assumptions (e.g., known HPI contexts). The Appendix §A.7 discusses the hyperparameter settings for the estimators in detail.



(a) Synthetic networks and one or more peer influence mechanisms



(b) Semi-synthetic networks and different peer influence mechanisms

Figure 5: Estimation error for IDEs with effect modification and heterogeneous peer influence (HPI).

## 6.2 Results

Here, we discuss the main takeaways from our experiments by showing a representative result and referring to additional results in Appendix A.1 (due to limited space).

**Our proposed method is robust when both treatment effect modification and HPI are present.** In the first experiment, we set the coefficient  $\tau_d = -1$  and vary coefficients  $\tau_a$  and  $\tau_n$  to generate ground truth IDEs due to effect modifications based on unit attributes and unit’s degree compared to peers. We enable HPI based on tie strength ( $\tau_{Z_r} = 1$ ), mutual connections ( $\tau_{E-r} = 1$ ), attribute similarity ( $\tau_{Z_{-i}} = 1$ ), or a linear combination of these contexts. We vary the strength of peer exposure  $\tau_p$  and run the experiment with three configurations of BA and WS networks with sparse to dense edge densities 15 times for each parameter setting. Figure 5(a) shows the  $\epsilon_{PEHE}$  with standard error for different network configurations averaged for all four HPI mechanisms. We observe our approach is robust to unknown HPI and effect modification but the baselines suffer high bias depending on network topology and edge density. Baselines incur higher bias for low heterogeneous peer exposure due to effect modification. Interestingly, the MLP-CFR baseline method has competitive performance for denser synthetic graphs for heterogeneous effects but biased average effects (Figure 8(a)). In Figure 5(b), we observe the performance of estimators for each underlying peer influence mechanism for two real-world networks. Our proposed approach has robust performance for all four mechanisms in both real-world networks. While IDE-TARNet-INT has slightly poor  $\epsilon_{PEHE}$  for synthetic data, it has competitive performance for semi-synthetic data. The non-GNN baseline BART-NET-INT, although computationally expensive, has decent performance on semi-synthetic data, consistent with previous observation (Guo, Li, and Liu 2020). BART is known to capture effect modifiers well (Hill 2011). Our method is robust for ATE estimation as well (Figure 8).

**Ignoring HPI results in biased heterogeneous and average direct effects.** In the second experiment, we evaluate

the estimation of constant direct effects  $\tau_d = -1$  for a similar setup as the first experiment. Here, we have no effect modifications to investigate bias only due to HPI. In Figure 6, we can observe the robustness of IDE-TARNet for both synthetic and semi-synthetic data settings. The baselines suffer high bias depending on network topology and edge density. For example, NetEst performs better for sparse networks but suffers for dense networks. Most baselines do well for the dense WS network because the heterogeneity contexts like mutual friend count are mostly homogeneous. Now, baselines have a comparatively low bias for low heterogeneous peer exposure due to the absence of effect modification. Figure 9 in §A.1 includes an ablation study to support the robustness of our embeddings for estimating individual effects when peer exposures are effect modifiers.

## 7 Main Takeaways and Discussion

We motivated and investigated the problem of estimating individual direct effects under unknown heterogeneous peer influence mechanisms. We proposed flexible models (NSCM and NAGG) to identify potential heterogeneous contexts as relational variables and an estimator (IDE-TARNet) for representation learning of these relational variables to estimate robust individual direct effects.

**Connections to other HPI work.** While our framework is not a replacement for related work dealing with specific HPI (Tran and Zheleva 2022; Yuan, Altenburger, and Kooti 2021; Qu et al. 2021; Ma et al. 2022), it is general enough to capture their sources of heterogeneity. For instance, Figure 9 in the Appendix compares IDE-TARNet with the causal network motifs approach designed to address HPI due to local neighborhood structure. We discuss the concrete mappings to each work in the Appendix A.2.

**Potential implications and societal impacts.** The implications of our work include identifying subpopulations with heterogeneous effects. The potential societal impacts could include designing targeted intervention policies or discovering intervention policies that maximize desired utility in online or offline social networks.

**Future research directions.** Our work can be extended to estimate peer and total effects but we need to address causal estimation with counterfactual peer exposures with unknown HPI contexts. Extending our approach to make it scalable to larger networks is the next step for practical applications and §A.2 discusses more on it. Future investigations could include utilizing NSCM to relax the assumption of pre-treatment network structure and study heterogeneity in complex interventions on or affecting network ties.

## References

- Albert, R.; and Barabási, A.-L. 2002. Statistical mechanics of complex networks. *Reviews of modern physics*, 74(1): 47.
- Aral, S. 2016. Networked experiments. *The Oxford handbook of the economics of networks*, 376–411.
- Arbour, D.; Garant, D.; and Jensen, D. 2016. Inferring network effects from observational data. In *Proceedings of the 22nd ACM SIGKDD International Conference on Knowledge Discovery and Data Mining*, 715–724.
- Aronow, P. M.; and Samii, C. 2017. Estimating average causal effects under general interference, with application to a social network experiment. *The Annals of Applied Statistics*, 11(4): 1912–1947.
- Athey, S.; and Imbens, G. 2016. Recursive partitioning for heterogeneous causal effects. *Proceedings of the National Academy of Sciences*, 113(27): 7353–7360.
- Bareinboim, E.; and Pearl, J. 2016. Causal inference and the data-fusion problem. *Proceedings of the National Academy of Sciences*, 113(27): 7345–7352.
- Bargagli-Stoffi, F. J.; Tortù, C.; and Forastiere, L. 2020. Heterogeneous Treatment and Spillover Effects under Clustered Network Interference. *arXiv preprint arXiv:2008.00707*.
- Barkley, B. G.; Hudgens, M. G.; Clemens, J. D.; Ali, M.; and Emch, M. E. 2020. Causal inference from observational studies with clustered interference, with application to a cholera vaccine study. *Annals of Applied Statistics*, 14(3): 1432–1448.
- Blei, D. M.; Ng, A. Y.; and Jordan, M. I. 2003. Latent dirichlet allocation. *Journal of machine Learning research*, 3(Jan): 993–1022.
- Cristali, I.; and Veitch, V. 2022. Using embeddings for causal estimation of peer influence in social networks. *Advances in Neural Information Processing Systems*, 35: 15616–15628.
- Fatemi, Z.; and Zheleva, E. 2023. Contagion Effect Estimation Using Proximal Embeddings. *arXiv preprint arXiv:2306.02479*.
- Forastiere, L.; Airolidi, E. M.; and Mealli, F. 2021. Identification and estimation of treatment and interference effects in observational studies on networks. *Journal of the American Statistical Association*, 116(534): 901–918.
- Getoor, L.; Friedman, N.; Koller, D.; Pfeffer, A.; and Taskar, B. 2007. Probabilistic relational models. *Introduction to statistical relational learning*, 8.
- Gilad, A.; Parikh, H.; Roy, S.; and Salimi, B. 2021. Heterogeneous Treatment Effects in Social Networks. *arXiv preprint arXiv:2105.10591*.
- Guo, R.; Li, J.; and Liu, H. 2020. Learning individual causal effects from networked observational data. In *Proceedings of the 13th International Conference on Web Search and Data Mining*, 232–240.
- Halloran, M. E.; and Struchiner, C. J. 1995. Causal inference in infectious diseases. *Epidemiology*, 142–151.
- Hayes, A.; Fredrickson, M. M.; and Levin, K. 2022. Estimating network-mediated causal effects via spectral embeddings. *arXiv preprint arXiv:2212.12041*.
- Heckerman, D.; Meek, C.; and Koller, D. 2007. Probabilistic entity-relationship models, PRMs, and plate models. *Introduction to statistical relational learning*, 2007: 201–238.
- Hill, J. L. 2011. Bayesian nonparametric modeling for causal inference. *Journal of Computational and Graphical Statistics*, 20(1): 217–240.
- Hudgens, M. G.; and Halloran, M. E. 2008. Toward causal inference with interference. *Journal of the American Statistical Association*, 103(482): 832–842.
- Jiang, S.; and Sun, Y. 2022. Estimating Causal Effects on Networked Observational Data via Representation Learning. In *Proceedings of the 31st ACM International Conference on Information & Knowledge Management*, 852–861.
- Johansson, F.; Shalit, U.; and Sontag, D. 2016. Learning representations for counterfactual inference. In *International conference on machine learning*, 3020–3029. PMLR.
- Kipf, T. N.; and Welling, M. 2016. Semi-Supervised Classification with Graph Convolutional Networks. In *International Conference on Learning Representations*.
- Künzel, S. R.; Sekhon, J. S.; Bickel, P. J.; and Yu, B. 2019. Metalearners for estimating heterogeneous treatment effects using machine learning. *Proceedings of the National Academy of Sciences*, 116(10): 4156–4165.
- Leavitt, H. J. 1951. Some effects of certain communication patterns on group performance. *The Journal of Abnormal and Social Psychology*, 46(1): 38.
- Lee, S. 2018. *Causal Discovery from Relational Data: Theory and Practice*. PhD thesis, The Pennsylvania State University.
- Lee, S.; and Honavar, V. 2015. Lifted representation of relational causal models revisited: implications for reasoning and structure learning. In *Proceedings of the UAI 2015 Conference on Advances in Causal Inference-Volume 1504*, 56–65.
- Lee, S.; and Honavar, V. 2016. A characterization of Markov equivalence classes of relational causal models under path semantics. In *Proceedings of the Thirty-Second Conference on Uncertainty in Artificial Intelligence*, 387–396.
- Lee, S.; and Honavar, V. 2020. Towards robust relational causal discovery. In *Uncertainty in Artificial Intelligence*, 345–355. PMLR.
- Ma, J.; Wan, M.; Yang, L.; Li, J.; Hecht, B.; and Teevan, J. 2022. Learning causal effects on hypergraphs. In *Proceedings of the 28th ACM SIGKDD Conference on Knowledge Discovery and Data Mining*, 1202–1212.
- Ma, Y.; and Tresp, V. 2021. Causal inference under networked interference and intervention policy enhancement. In *International Conference on Artificial Intelligence and Statistics*, 3700–3708. PMLR.
- Maier, M. 2014. Causal discovery for relational domains: Representation, reasoning, and learning. *PhD thesis, University of Massachusetts, Amherst*.



- Maier, M.; Marazopoulou, K.; Arbour, D.; and Jensen, D. 2013. A sound and complete algorithm for learning causal models from relational data. In *Proceedings of the Twenty-Ninth Conference on Uncertainty in Artificial Intelligence*, 371–380.
- Maier, M.; Taylor, B.; Oktay, H.; and Jensen, D. 2010. Learning causal models of relational domains. In *Proceedings of the AAAI Conference on Artificial Intelligence*, volume 24, 531–538.
- McNealis, V.; Moodie, E. E.; and Dean, N. 2023. Doubly Robust Estimation of Causal Effects in Network-Based Observational Studies. *arXiv preprint arXiv:2302.00230*.
- Nabi, R.; Pfeiffer, J.; Charles, D.; and Kıcıman, E. 2022. Causal inference in the presence of interference in sponsored search advertising. *Frontiers in big Data*, 5.
- Ogburn, E. L.; Shpitser, I.; and Lee, Y. 2020. Causal inference, social networks and chain graphs. *Journal of the Royal Statistical Society Series A: Statistics in Society*, 183(4): 1659–1676.
- Ogburn, E. L.; Sofrygin, O.; Diaz, I.; and Van der Laan, M. J. 2022. Causal inference for social network data. *Journal of the American Statistical Association*, 1–15.
- Ogburn, E. L.; and VanderWeele, T. J. 2014. Causal diagrams for interference. *Statistical science*, 29(4): 559–578.
- Patacchini, E.; Rainone, E.; and Zenou, Y. 2017. Heterogeneous peer effects in education. *Journal of Economic Behavior & Organization*, 134: 190–227.
- Pearl, J. 1988. *Probabilistic Reasoning in Intelligent Systems: Networks of Plausible Inference*. Morgan Kaufmann.
- Pearl, J. 2009. *Causality*. Cambridge university press.
- Pearl, J. 2010. Brief report: On the consistency rule in causal inference:” Axiom, definition, assumption, or theorem?”. *Epidemiology*, 872–875.
- Qidong, L.; Feng, T.; Weihua, J.; and Qinghua, Z. 2020. A new representation learning method for individual treatment effect estimation: Split covariate representation network. In *Asian Conference on Machine Learning*, 811–822. PMLR.
- Qu, Z.; Xiong, R.; Liu, J.; and Imbens, G. 2021. Efficient Treatment Effect Estimation in Observational Studies under Heterogeneous Partial Interference. *arXiv preprint arXiv:2107.12420*.
- Rubin, D. B. 1974. Estimating causal effects of treatments in randomized and nonrandomized studies. *Journal of educational Psychology*, 66(5): 688.
- Rubin, D. B. 1980. Randomization analysis of experimental data: The Fisher randomization test comment. *Journal of the American statistical association*, 75(371): 591–593.
- Salimi, B.; Parikh, H.; Kayali, M.; Getoor, L.; Roy, S.; and Suciu, D. 2020. Causal relational learning. In *Proceedings of the 2020 ACM SIGMOD international conference on management of data*, 241–256.
- Shalit, U.; Johansson, F. D.; and Sontag, D. 2017. Estimating individual treatment effect: generalization bounds and algorithms. In *International Conference on Machine Learning*, 3076–3085. PMLR.
- Shalizi, C. R.; and Thomas, A. C. 2011. Homophily and contagion are generically confounded in observational social network studies. *Sociological methods & research*, 40(2): 211–239.
- Shpitser, I.; Tchetgen, E. T.; and Andrews, R. 2017. Modeling interference via symmetric treatment decomposition. *arXiv preprint arXiv:1709.01050*.
- Toulis, P.; and Kao, E. 2013. Estimation of causal peer influence effects. In *International conference on machine learning*, 1489–1497. PMLR.
- Tran, C.; and Zheleva, E. 2022. Heterogeneous Peer Effects in the Linear Threshold Model. *Proceedings of the AAAI Conference on Artificial Intelligence*.
- Ugander, J.; Karrer, B.; Backstrom, L.; and Kleinberg, J. 2013. Graph cluster randomization: Network exposure to multiple universes. In *Proceedings of the 19th ACM SIGKDD international conference on Knowledge discovery and data mining*, 329–337.
- Veličković, P.; Cucurull, G.; Casanova, A.; Romero, A.; Liò, P.; and Bengio, Y. 2018. Graph Attention Networks. In *International Conference on Learning Representations*.
- Watts, D. J.; and Strogatz, S. H. 1998. Collective dynamics of ‘small-world’ networks. *nature*, 393(6684): 440–442.
- Xu, K.; Hu, W.; Leskovec, J.; and Jegelka, S. 2018. How Powerful are Graph Neural Networks? In *International Conference on Learning Representations*.
- Yuan, Y.; Altenburger, K.; and Kooti, F. 2021. Causal Network Motifs: Identifying Heterogeneous Spillover Effects in A/B Tests. In *Proceedings of the Web Conference 2021*, 3359–3370.
- Zhang, C.; Mohan, K.; and Pearl, J. 2022. Causal inference with non-IID data using linear graphical models. *Advances in Neural Information Processing Systems*, 35: 13214–13225.

## A Appendix

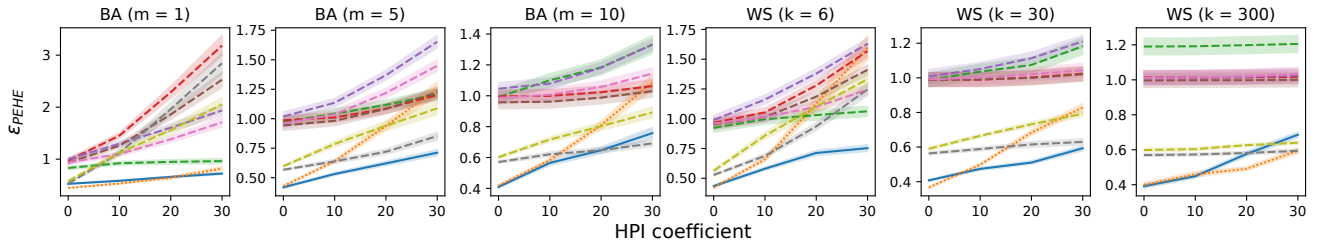
### A.1 Main results (continued...)

This section shows Figures 6, 7, and 8 referenced and discussed in the main paper. These results, along with Figure 5 in the main paper, establish the robustness of our proposed estimator when heterogeneous peer influence (HPI) acts as a nuisance or bias in the estimation of direct individual causal effects. For experimental settings in Figures 5–8, IDE (as defined in Equation 2) are equivalent to "insulated" individual effects (Jiang and Sun 2022) because influences from peers do not interact with the treatment assignments of individuals. The robustness of our method, IDE-TARNet, for estimating heterogeneous and average effects in the presence of HPI and effect modification due to contexts related to individual attributes and network position is demonstrated in Figures 5 and 8, respectively. Figures 6 and 7 illustrate the effectiveness of our methods when the underlying IDEs are constant but the peer influence is heterogeneous.

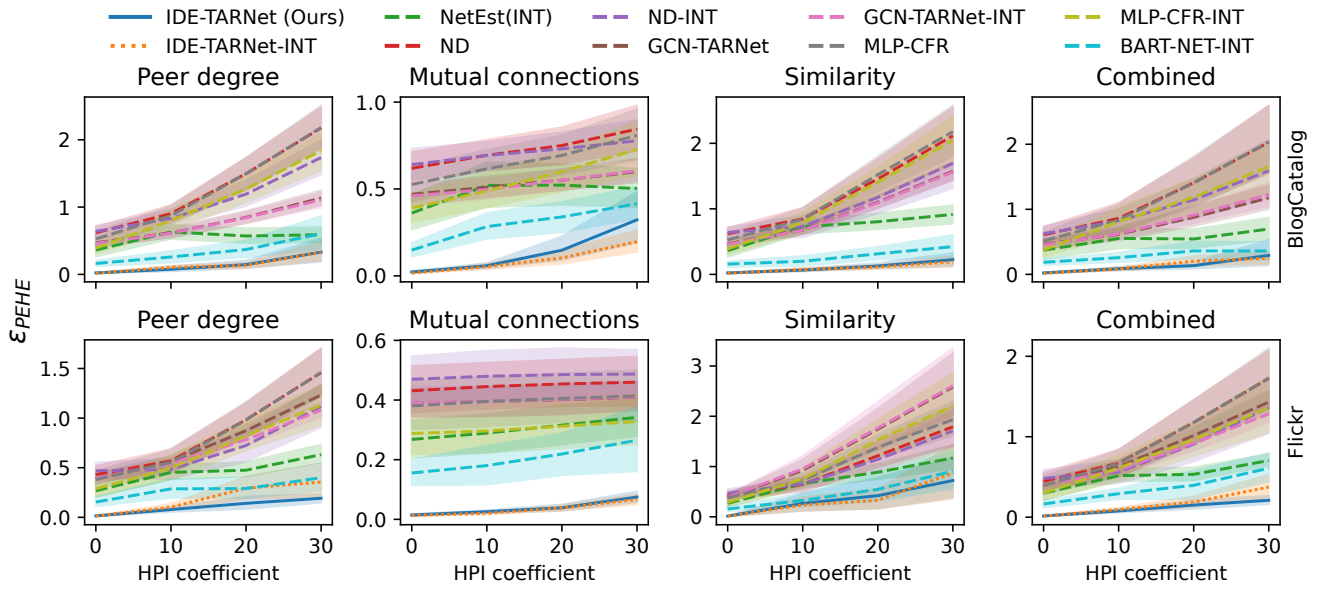
Figure 9 shows the results of a follow-up experimental setting when there is effect modification due to peer exposure and the true IDEs capture heterogeneous influences from peers as referenced (but not discussed) in §6.2. We generate the outcome as  $Y_i = f_Y(\tau_p\phi(X_{-i}, \mathcal{Z}_i) + \tau_p\phi(X_{-i}, \mathcal{Z}_i)X_i + \dots)$ , where "... " denotes other terms,  $\tau_p$  is the peer exposure coefficient, and  $\phi(X_{-i}, \mathcal{Z}_i)$  capture strength of peer exposure due to some underlying mechanism. The true IDEs in this setting are  $\tau_p\phi(X_{-i}, \mathcal{Z}_i)$  and we evaluate how well the estimators estimate the IDE with the  $\epsilon_{PEHE}$  metric. The IDEs in this setting are different from "insulated" individual causal effects (Jiang and Sun 2022) due to the interaction with peer exposure. This experimental setting also acts as an **ablation study** to examine the contributions of our feature and exposure embeddings. In previous experimental settings, we used the baseline estimators and mostly default hyperparameters (see §A.7 for details) implemented in the NetEst (Jiang and Sun 2022) and Network Deconfounder (ND) (Guo, Li, and Liu 2020) papers. Here, baselines also use counterfactual prediction modules and hyperparameters like our IDE-TARNet estimator. We use GCN-TARNet and GCN-CFR with causal network motifs (Yuan, Altenburger, and Kooti 2021) as exposure embeddings for baselines instead of NetEst (Jiang and Sun 2022), which performs poorly for IDE estimation. The poor performance may be because NetEst is designed for "insulated" individual effect estimation (Jiang and Sun 2022) and concatenates the treatment assignment to the feature and exposure embeddings instead of using a treatment-agnostic approach (Shalit, Johansson, and Sontag 2017).

Causal network motifs (Yuan, Altenburger, and Kooti 2021) capture recurrent subgraphs with treatment assignments to represent heterogeneous peer exposure based on local neighborhood structure. Let the symbol  $\bullet$  indicate the treated peer and  $\circ$  indicate the peer in the control group. In the ego's neighborhood, we use normalized counts of dyads ( $\{\circ\}$ ,  $\{\bullet\}$ ), open triads ( $\{\bullet\bullet\}$ ,  $\{\bullet\circ\}$ ,  $\{\circ\circ\}$ ), and closed triads ( $\{\bullet-\bullet\}$ ,  $\{\bullet-\circ\}$ ,  $\{\circ-\circ\}$ ) to construct the exposure embedding following Yuan, Altenburger, and Kooti (2021). We compare our method IDE-TARNet (with smoothing regularization) against GCN-TARNet (with no regularization) and GCN-CFR (with representation balancing regularization (Shalit, Johansson, and Sontag 2017; Guo, Li, and Liu 2020)) consisting causal motif fractions (MOTIFS) or a fraction of treated peers (HOM-INT) or no exposure embeddings. We also include IDE-TARNet-INT (with smoothing regularization) as a baseline for the ablation study. We generate heterogeneous peer influence due to influence mechanisms like mutual connections, attribute similarity, tie strength, and peer degree, as discussed in the main paper. Additionally, we include structural diversity as an underlying influence mechanism that considers the number of connected components among treated peers as peer exposure (Yuan, Altenburger, and Kooti 2021). We use peer exposure coefficient  $\tau_p = 1$  for structural diversity and  $\tau_p = 20$  for other influence mechanisms. Figure 9 shows the performance of proposed and baseline estimators for synthetic scale-free (BA) and small-world (WS) networks with different edge densities. Due to the computational cost of extracting exposure embeddings with causal network motifs, we use a WS graph with a cluster size of  $K = 15$  instead of  $K = 300$  in the previous settings.

We observe in Figure 9 that causal motifs capture peer influences due to structural diversity (with open triads) and mutual connections (with closed triads) well. However, as expected, causal motifs cannot capture peer influences due to attribute similarity, tie strength, and peer degree in scale-free networks with a non-uniform degree distribution. IDE-TARNet on the other hand is robust for different underlying peer influence mechanisms and competitive to causal motifs for structural diversity and mutual connection mechanisms. Estimators assuming homogeneous influence suffer high bias unless the network topology and influence mechanisms produce uniform influences (e.g., peer degree in small-world networks). Estimators assuming no network interference have a large bias in every setting when there is effect modification due to peer exposure.

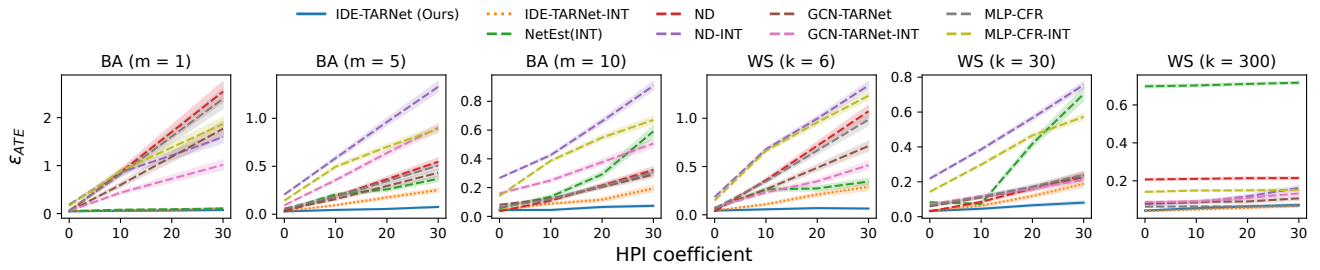


(a) Synthetic networks and one or more peer influence mechanisms

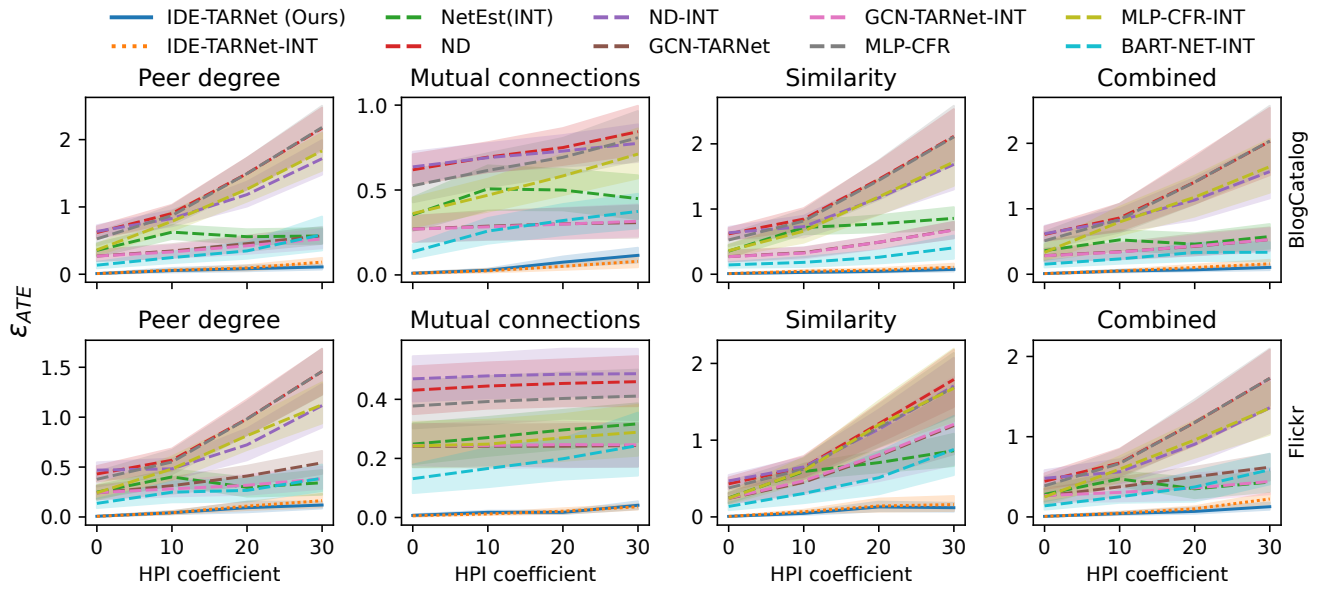


(b) Semi-synthetic networks and different peer influence mechanisms

Figure 6:  $\epsilon_{PEHE}$  errors for **constant true individual direct effects** and heterogeneous peer influence.

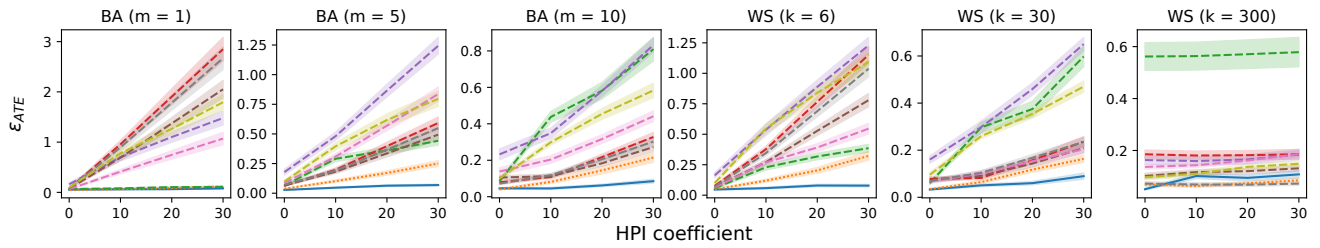


(a) Synthetic networks and one or more peer influence mechanisms

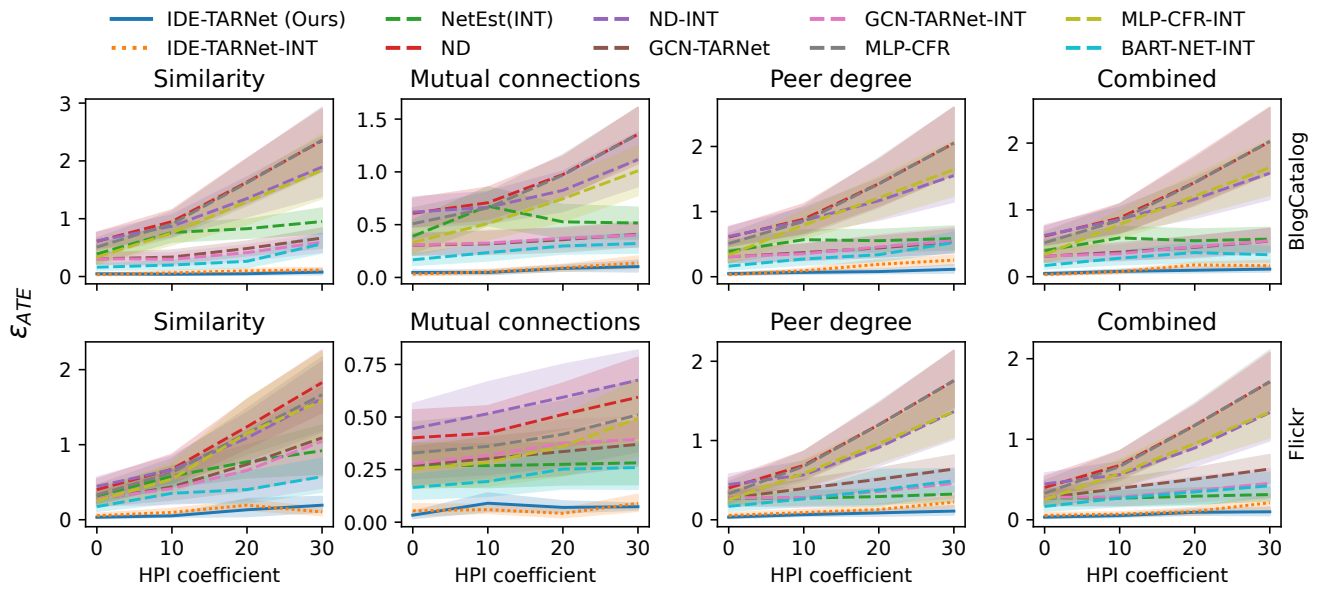


(b) Semi-synthetic networks and different peer influence mechanisms

Figure 7:  $\epsilon_{ATE}$  errors for **constant true individual direct effects** and heterogeneous peer influence.



(a) Synthetic networks and one or more peer influence mechanisms



(b) Semi-synthetic networks and different peer influence mechanisms

Figure 8:  $\epsilon_{ATE}$  errors for individual direct effects with effect modification and heterogeneous peer influence.

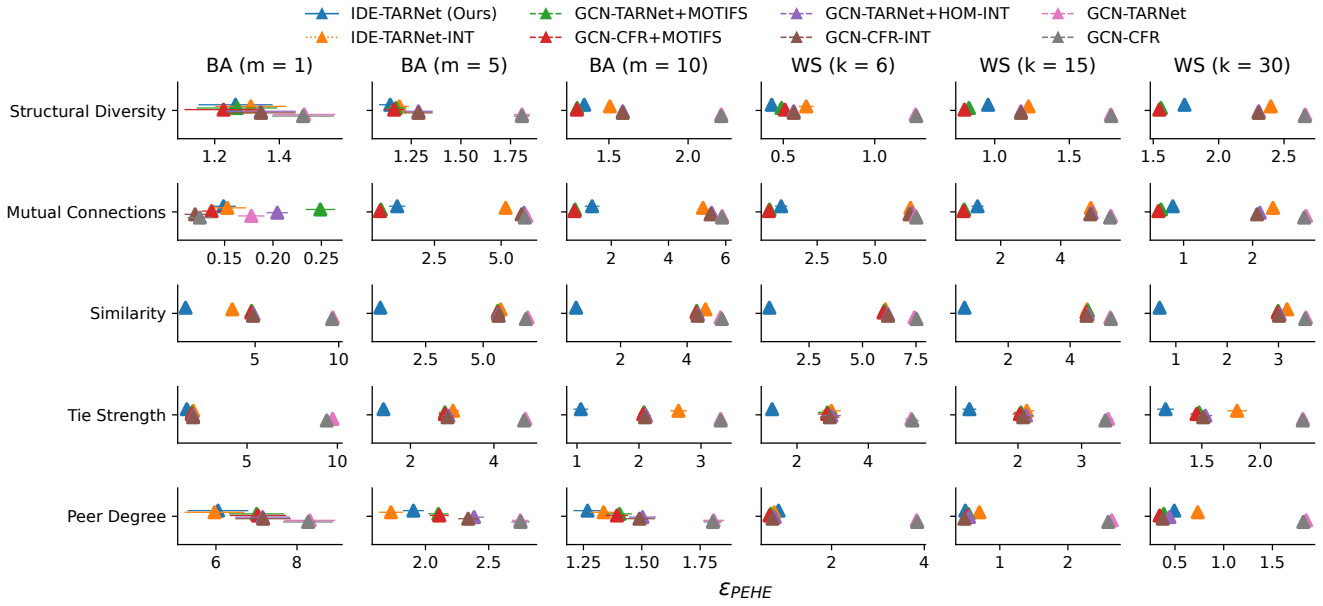


Figure 9:  $\epsilon_{PEHE}$  errors, for different underlying heterogeneous peer influence mechanisms and synthetic networks with different topologies and edge densities, when **the peer exposure is an effect modifier** and defines individual effects. While causal motifs capture peer influences due to structural diversity and mutual connections well, they cannot capture peer influences due to attribute similarity, tie strength, and peer degree in scale-free networks with a non-uniform degree distribution. IDE-TARNet, on the other hand, is robust for different underlying peer influence mechanisms and competitive to causal motifs for structural diversity and mutual connection mechanisms.

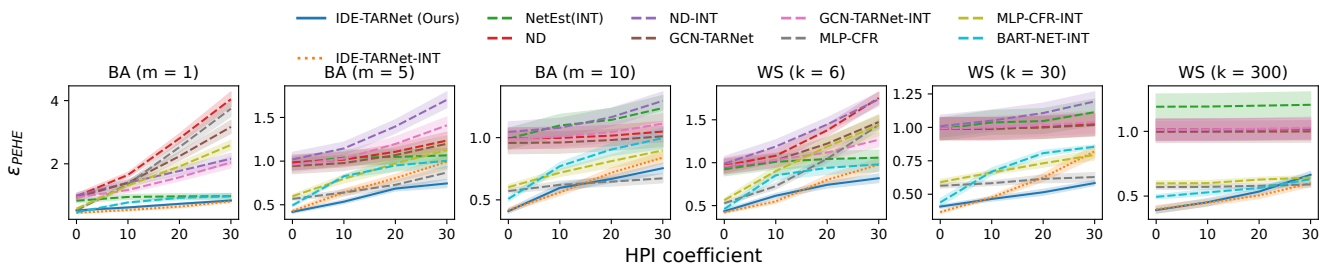


Figure 10:  $\epsilon_{PEHE}$  errors for individual direct effects with effect modification (EM) and heterogeneous peer influence (HPI) due to combined contexts in Synthetic data. Although the performance of BART-NET-INT for synthetic data with EM under HPI is comparable to better baselines, our method is consistently more robust.

## A.2 Discussion

**Connections to other HPI work.** We characterize existing work based on peer influence mechanisms as approaches considering homogeneous influence, known heterogeneous influence, or specific heterogeneous mechanisms. However, these works have different scopes and solve different problems. Our work highlights the importance of modeling unknown heterogeneous peer influence mechanisms for individual direct effect estimation. While our framework is not a replacement for existing approaches dealing with specific HPI (Tran and Zheleva 2022; Yuan, Altenburger, and Kooti 2021; Qu et al. 2021; Ma et al. 2022), it is general enough to capture their sources of heterogeneity. Moreover, these approaches could use our work to cover additional sources of heterogeneity. For instance, Figure 9 in the Appendix compares IDE-TARNet with the causal network motifs approach designed to address HPI due to local neighborhood structure. IDE-TARNet leverages graph convolution networks (GCN) and triangle counts ( $AA^T$ ) for exposure embeddings to capture the representation of local neighborhoods. Other sources of heterogeneity due to variable susceptibilities of units (Tran and Zheleva 2022) and unit’s covariates (Qu et al. 2021) are captured by node attributes while group interactions captured with hypergraphs (Ma et al. 2022) could be modeled by IDE-TARNet with either node or edge attributes.

**Scalability.** Extending our approach to make it scalable to larger networks is the next step for practical applications. A potential solution could rely on capturing 1-hop neighborhoods for each node vs. needing to feed the full network, as the current solution does. Let  $N$ ,  $M$ , and  $D$ , respectively denote the number of nodes, edges, and the dimension of features or representations. The scalability of the current approach, like GCN, depends on time complexity  $O(ND^2)$  for feature transformation and  $O(MD)$ , the number of edges (mostly linearly given constant dimension) for peer aggregation because we use sparse matrix multiplication whose complexity depends on the number of non-zero elements in the adjacency matrix ( $A$ ). However, one term  $AA^T$  in the exposure mapping introduced to explicitly capture structural property (number of walks of the path two between  $v_i$  and  $v_j$ ) incurs time complexity of  $O(MN)$ . This time complexity and overall space complexity can be improved by using batches of ego-network and ongoing work to apply our framework to large real-world networks for discovering populations with heterogeneous effects is addressing the scalability. The scope of the current work focuses on evaluating different network and data generation settings for IDE estimation under HPI.

## A.3 Feature and exposure embeddings

**Feature embeddings.** We propose GNN feature embeddings  $h_f$  by concatenating outputs of ego multi-layer perception (MLP)  $h_i$ , the peer graph convolution network (GCN)  $h_{-i}$ , and edge GCN  $h_r$  modules capturing relational variables  $\phi_i(Z_i)$ ,  $\phi_{-i}(Z_{-i}, E_r)$ , and  $\phi_r(Z_r, Z_{-r}, E_r, E_{-r})$ , respectively. Let  $\Theta$  denote MLP with ReLU, then

$$h_i = \Theta(\mathbf{Z}_n), h_{-i} = \mathbf{D}^{-\frac{1}{2}} \mathbf{A} \Theta(\mathbf{Z}_n), h'_r = \sum^{row} \mathbf{A} \odot \Theta(\mathbf{Z}_e), h_r = h'_r \|\mathbf{D}^{-\frac{1}{2}} \mathbf{A} h'_r, \text{ and } h_f = h_i \| h_{-i} \| h_r,$$

where  $\mathbf{D}$  is a degree matrix used for normalization,  $\odot$  is index-wise product operator, and  $\|$  is a concatenation operator. Here,  $h_{-i}$  is a normalized GCN and  $h_r$  is GCN after peer aggregation ( $h'_r$ ). Existing work has shown mean aggregation, i.e., normalization using  $\mathbf{D}^{-1}$  could make GNNs less expressive than sum aggregation (Xu et al. 2018). However, using the sum aggregation may make representations unstable, especially in scale-free networks (e.g., online social networks) that have some nodes with high degrees, and we choose  $\mathbf{D}^{-\frac{1}{2}}$  for normalization.

**Exposure embeddings.** Let  $\langle \mathbf{v}_i, \mathbf{v}_j \rangle$  be the indices of nodes with edges, i.e., non-zero  $\mathbf{A}$ , then, we define exposure embedding  $h_e$  as a weighted mean, i.e.,

$$h_e = \frac{\sum^{row} \mathbf{A} \odot h_w \odot X_i[\mathbf{v}_j]}{\sum^{row} \mathbf{A} \odot h_w} |_{h_w} := \Theta(\mathbf{Z}_e) \| (\mathbf{A} \odot (\mathbf{A} \mathbf{A}^T)) [\mathbf{v}_i, \mathbf{v}_j] \| h_f[\mathbf{v}_i] \| sim(h_f[\mathbf{v}_i], h_f[\mathbf{v}_j]),$$

where  $h_w \in \mathbb{R}^{m \times k}$  represents edge weights capturing underlying peer influence strength,  $[\cdot]$  indicates indexing, and  $sim(a, b) = e^{-(a-b)^2}$  captures similarity. The edge attributes, network connections, peer features, and similarity with peers are incorporated in  $h_w$  as potential influence strengths.

## A.4 Data generation

First, we discuss the data generation for confounder  $C_i$ , context  $Z_i$ , and tie strength  $Z_r$  for synthetic data as referenced in §6.1. We generate  $C_i \sim Beta(0.6, 0.6)$  to model demographics predictive of political polarity,  $Z_i \sim Categorical(K = 5, \mathbf{p} \sim Dirichlet(5, 5, 5, 5, 5))$  to model membership in one of five demographic subgroups, and  $Z_r \sim Uniform(1, 10)$  to model friendship duration as tie strength. Here, the *Beta* distribution with the parameters gives values in the range  $(0, 1)$  with a slightly polar distribution most values near 0 and 1 as fewer values toward 0.5. The *Dirichlet* distribution gives probabilities values that sum to 1 for the *Categorical* distribution.

**Treatment model.** For observational data, a unit’s treatment may be influenced by its own covariates as well as the treatments or covariates of other units, depending on the interference conditions. We generate treatment  $X_i$  for unit  $v_i$  as  $X_i \sim \theta(a(\tau_c \mathbf{W}_x \cdot \frac{\sum E_r \odot C_{-i}}{\sum E_r} + (1 - \tau_c) \mathbf{W}_x \cdot C_i))$ , where  $\theta$  denotes Bernoulli distribution,  $a : \mathbb{R} \mapsto [0, 1]$  is an activation function,  $\tau_c \in [0, 1]$  controls spillover influence from unit  $v_i$ ’s peers, and  $\mathbf{W}_x$  is the weight matrix.

**Outcome model.** We define unit  $v_i$ ’s outcome  $Y_i$  as a function of unit’s treatment ( $\tau_d$ ), unit’s attribute effect modifier ( $\tau_a$ ), network effect modifier ( $\tau_n$ ), heterogeneous influence from peers ( $\tau_p, \tau_{Z_r}, \tau_{Z_{-i}}, \tau_{E_{-r}}$ ), confounder ( $\tau_{c1}$ ), and random noise

$(\epsilon \sim \mathcal{N}(0, 1))$ .

$$Y_i = \tau_0 + \tau_{c1}C_i + \tau_d X_i + \tau_a X_i Z_i + \tau_n X_i \mathbb{1}[(\sum E_r) > g_p(E_{-r})] + \epsilon + \tau_p X_{-i} \cdot g_n(\tau_{Z_r} \cdot \phi(Z_r) + \tau_{Z_{-i}} \cdot \phi(E_r \odot rbf(Z_i, Z_{-i})) + \tau_{E_{-r}} \cdot \phi(E_r \odot g(E_r, E_{-r}))), \quad (3)$$

where  $\tau_0$  is a constant,  $g_p$  gives  $p^{th}$  percentile value of peers' degree  $g(E_{-r})$ ,  $g_n(\vec{Z}) = \frac{\vec{Z}}{\sum \vec{Z}}$  gives normalized weight,  $\phi(Z)$  is one of  $\{Z^2, \sqrt{Z}, Z\}$ , and  $rbf$  is a radial basis function. The coefficients  $\tau_a$  and  $\tau_n$  control treatment effect modification based on node attributes (e.g., age group) and network location (e.g., degree centrality), respectively. We model variable influence from peers based on the strength of ties ( $\tau_{Z_r}$ ), the attribute similarity and friendship existence ( $\tau_{Z_{-i}}$ ), local structure captured by the count of mutual friends ( $\tau_{E_{-r}}$ ), and peer exposure coefficient ( $\tau_p$ ).

The generated data is used in the treatment and outcome models. For synthetic data, we use  $\tau_c = 0.5$  in the treatment model to control spillover from peers' confounders. Similarly, we use weight matrix  $\mathbf{W}_x = 1$  and identity activation  $a$  in the treatment model to generate treatment assignment  $X_i$ . For the outcome model, we use the square of tie strength and the square root of mutual friend count to introduce non-linear influences in the underlying model. The radial basis function in the outcome model uses  $gamma = 2$ .

For the semi-synthetic data, we randomly assign 50-dimensional features of each unit to confounders or effect modifiers. Confounders are the features that affect both treatment and outcome whereas effect modifiers (except confounders) do not affect the treatment. We generate masks drawn from the Bernoulli distribution and weights drawn from the uniform distribution to get weights  $\mathbf{W}_x$  and  $\mathbf{W}_y$  for all 50-dimensional features, i.e.,

$$\begin{aligned} M_x &\sim \text{Bernoulli}(0.6), \\ M_y &\sim \text{Bernoulli}(0.6), \\ W_x &\sim M_x \times \text{Uniform}(-3, 3), \text{ and} \\ W_y &\sim M_y \times \text{Uniform}(-3, 3). \end{aligned}$$

The treatment model for semi-synthetic data is similar to that of synthetic data except we use the weights  $\mathbf{W}_x$  and activation function  $a$  is Sigmoid, i.e.,

$$X_i \sim \theta(\text{Sigmoid}(\tau_c \mathbf{W}_x \cdot \frac{\sum E_r \odot C_{-i}}{\sum E_r} + (1 - \tau_c) \mathbf{W}_x \cdot C_i)),$$

where  $C_i$  represent the 50-dimensional features. The outcome model is similar to the synthetic data but we multiply  $C_i$  with  $\mathbf{W}_y$  and we include features with  $M_x = 0$  and  $M_y = 1$  to  $Z_i$ .

## A.5 Proofs for NSCM and NAGG

The proof for Lemma 1, similar to Arbour, Garant, and Jensen (2016), is as follows:

*Proof.* Proof by contradiction. Let  $P = [I, \dots, I_k]$  and  $Q = [I, \dots, I_l]$  be two distinct relational paths sharing base item class  $I \in \{E, R\}$ . Assume for contradiction that  $P$  and  $Q$  intersect such that their terminal sets  $P|_{i \in \sigma(I)} \cap Q|_{i \in \sigma(I)} \neq \phi$ . Since we know both  $P$  and  $Q$  share base item class and are two different paths, one path is a prefix of another path for the SESR model. According to the bridge burning semantics, terminal set of prefix path is not visited again by the other path. This contradicts with the previous assumption. Therefore  $P$  and  $Q$  do not intersect.  $\square$

The proof for Proposition 1 is as follows:

*Proof.* Let  $S = (E, R, A)$  be a relational schema for a single-entity and single-relationship (SESR) model with arbitrary skeleton  $\sigma \in \Sigma_S$ . For enabling relationship existence uncertainty, Definition 1 defines relational skeleton in terms of entity instances  $\sigma(E)$  and fully-connected relationship instances  $\sigma(R) = \Sigma_{\sigma(E)}$ . Let  $N = |\sigma(E)|$ , then there are  $|\sigma(R)| = \frac{N \times N - 1}{2}$  relationship instances connecting each entity instance with other entities instances. Let us consider an arbitrary path  $\hat{P} = [I_j, \dots, I_k]$  to be traversed under bridge burning semantics (BBS).

*Claim 1.*  $P|_{I_j \in E}$  has a maximum length of valid relational path of four.

*Proof.* As illustrated in Figure 1, the terminal set for  $P|_{i_j \in \sigma(E)}$  has 1 entity instance for path  $E$ ,  $N - 1$  relationship instances for path  $[E, R]$ ,  $N - 1$  entity instances for path  $[E, R, E]$ , and remaining  $|\sigma(R)| - (N - 1)$  relationship instances for path  $[E, R, E, R]$ . By this point all entity and relationship instances are visited and path  $[E, R, E, R, E]$  produces an empty terminal set, making it an invalid path.  $\square$

*Claim 2.*  $P|_{I_j \in R}$  has a maximum length of valid relational path of five.

*Proof.* Similar to Claim 1, the terminal set for  $P|_{i_j \in \sigma(R)}$  has 1 relationship instance for path  $R$  and two entity instances for path  $[R, E]$ . Next, the terminal set for path  $[R, E, R]$  consists of  $2 \times N - 2$  relationship instances. The terminal sets from previous level connect to remaining  $N - 2$  entity instances for path  $[R, E, R, E]$ . Finally, the terminal set for path  $[R, E, R, E, R]$  traverses remaining relationship instances. By this point all entity and relationship instances are visited and path  $[R, E, R, E, R, E]$  produces empty terminal set, making it an invalid path.  $\square$



□

Here, we present formal definition of ground graph following Maier (2014)'s definition.

**Definition 4** (Ground graph). A *ground graph*  $GG_{\mathcal{M}\sigma}(V, E)$  is a realization of the NSCM  $\mathcal{M}(S, \mathbf{D}, \mathbf{f})$  for skeleton  $\sigma$  with nodes  $V = \{i.X \mid i \in \sigma(I) \wedge X \in \mathcal{A}(I)\}$  and edges  $E = \{i_k.X \rightarrow i_j.Y \mid [I_j, \dots, I_k].X \rightarrow [I_j].Y \in \mathbf{D} \wedge i_k \in [I_j, \dots, I_k]_{i_j}^\sigma \wedge \{i_k.X, i_j.Y\} \in V\}$ .

The proof for Theorem 1 follows the proof by Maier (2014) and is provided below:

*Proof.* Let  $\mathcal{M}(S, \mathbf{D})$  be an arbitrary acyclic NSCM and let  $B \in \{E, R\}$  be an arbitrary perspective. As a consequence of Lemma 1 and Proposition 1,  $NAGG_{\mathcal{M}B}$  does not have intersection variables and contains limited relational variables. Let  $P_k = [B, \dots, I_k]$  and  $P_j = [B, \dots, I_j]$  be two arbitrary valid paths for perspective  $B$ .

**Soundness:** To prove the soundness of  $NAGG_{\mathcal{M}B}$ , we must show that for every edge  $P_k.X \rightarrow P_j.Y$  in the  $NAGG_{\mathcal{M}B}$ , there exist a corresponding edge  $i_k.X \rightarrow i_j.Y \mid \exists b \in \sigma(B), i_k \in P_k|_b \wedge i_j \in P_j|_b$  in the ground graph  $GG_{\mathcal{M}\sigma}$  for some skeleton  $\sigma \in \Sigma_S$ . By construction, for the perspective  $B = E$ , any skeleton with  $N \geq 3$ , where  $N = |\sigma(E)|$ , has all possible paths  $[E], [E, R], [E, R, E]$ , and  $[E, R, E, R]$  with non-empty terminal sets, making them valid paths (Proposition 1). Similarly, for  $B = R$ , any skeleton with  $N \geq 4$  has all possible paths  $[R], [R, E], [R, E, R], [R, E, R, E]$ , and  $[R, E, R, E, R]$  with non-empty terminal sets, making them valid paths. This shows the existence of  $b \in \sigma(B)$  with  $i_k \in P_k|_b \wedge i_j \in P_j|_b$  for some skeleton  $\sigma \in \Sigma_S$ .

Assume for contradiction, there exists no edge  $i_k.X \rightarrow i_j.Y$  in any ground graph i.e.,  $\forall \sigma \in \Sigma_S \forall b \in \sigma(B) \forall i_k \in [B, \dots, I_k]|_b \forall i_j \in [B, \dots, I_j]|_b, i_k.X \rightarrow i_j.Y \notin GG_{\mathcal{M}\sigma}$ . However, according to the definition of  $NAGG_{\mathcal{M}B}$ , if the relational edge  $[B, \dots, I_k].X \rightarrow [B, \dots, I_j].Y$  is present, then there must be a dependency  $[I_j, \dots, I_k].X \rightarrow [I_j].Y \in \mathbf{D}$  where  $[B, \dots, I_k] \in \text{extend}([B, \dots, I_j], [I_j, \dots, I_k])$ . This implies the ground graphs must have an edge such that:

$$\forall \sigma \in \Sigma_S \forall i_j \in \sigma(I_j) \forall i_k \in [I_j, \dots, I_k]_{i_j}, i_k.X \rightarrow i_j.Y \in GG_{\mathcal{M}\sigma}.$$

Since  $[B, \dots, I_j]$  is a valid path, we know  $\exists i_j \in \sigma(I_j), i_j \in [B, \dots, I_j]|_b$ . To contradict the previous assumption, we prove the following Lemma about sufficient and necessary conditions for the soundness of *extend* (Maier 2014) operator:

**Lemma 3.** *If  $[B, \dots, I_k] \in \text{extend}([B, \dots, I_j], [I_j, \dots, I_k])$ , then the following must be true:*

$$\exists i_j \in [B, \dots, I_j]|_b \exists i_k \in [I_j, \dots, I_k]_{i_j}, i_k \in [B, \dots, I_k]|_b \wedge \forall S \in \mathbf{P}_B \setminus \{[B, \dots, I_k]\}, i_k \notin S|_b,$$

where  $\mathbf{P}_B$  is a set of valid paths for the perspective  $B$ .

*Proof.* (1) Sufficient condition (Lee 2018):  $i_k \in [B, \dots, I_k]|_b$ .

The proof follows directly from definition of *extend* and Maier (2014)'s Lemma 4.4.1. Let  $P_o = [B, \dots, I_j]$  and  $P_e = [I_j, \dots, I_k]$  denote original and extension paths. The *extend* function is defined as follows:

$$\text{extend}(P_o, P_e) = \{P = P_o^{1:n_o-i+1} + P_e^{i+1:n_e} \mid i \in \text{pivots}(\text{reverse}(P_o), P_e) \wedge \text{isValid}(P)\}, \text{ with } \text{pivots}(P_1, P_2) = \{i \mid P_1^{1:i}, P_2^{1:i}\},$$

where  $n_o = |P_o|$ ,  $n_e = |P_e|$ ,  $P^{i:j}$  is  $i$ -inclusive and  $j$ -inclusive path slicing,  $+$  denotes path concatenation, and *reverse* is a function that reverses the order of a path. Let  $c \in \text{pivots}(\text{reverse}(P_o), P_e)$  be a value obtained after applying the *pivots* function, then there are two subcases:

(a)  $c = 1$  and  $P = [B, \dots, I_j, \dots, I_k]$ . Since  $P$  is a valid path, the terminal set is not empty i.e.,  $\exists i_k \in \sigma(I_k), P|_b$ . As  $I_j$  is in the intermediate path,  $\exists i_j \in [B, \dots, I_j]|_b \exists i_k \in [I_j, \dots, I_k]_{i_j}, i_k \in P|_b$  for  $P|_b$  to be non-empty.

(b)  $c > 1$  and  $P = [B, \dots, I_c, \dots, I_k]$ . We must have  $P_o = [B, \dots, I_c, \dots, I_j]$  and  $P_e = [I_j, \dots, I_c, \dots, I_k]$  for pivot  $c > 1$  to produce  $P$ . Similar to case (a), since  $P$  is a valid path, the terminal set is not empty i.e.,  $\exists i_k \in \sigma(I_k), P|_b$ . Also, we know from case (a),  $\exists i_c \in [B, \dots, I_c]|_b \exists i_k \in [I_c, \dots, I_k]_{i_c}, i_k \in P|_b$ . We then must show that  $\exists i_j \in [I_c, \dots, I_j]_{i_c}, i_c \in [I_j, \dots, I_c]_{i_j}$ . The fully connected skeleton with  $N = |\sigma(E)|$  entity instances and  $|\sigma(R)| = \frac{N \times N - 1}{2}$  relationship instances according to Definition 1 allows traversal from  $i_c$  to  $i_j$  and vice versa.

(2) Necessary condition (Lee 2018):  $\forall S \in \mathbf{P}_B \setminus \{[B, \dots, I_k]\}, i_k \notin S|_b$

Lee (2018) points out this necessary condition is required to ensure the parents of  $[B, \dots, I_j].Y$  should not be redundant and propose a method called *newextend* for handling both necessary and sufficient conditions. Here, we show that the *extend* method satisfies necessary condition as well for  $NAGG_{\mathcal{M}B}$ . Suppose for contradiction the necessary condition is false. This means the item  $i_k$  appears in the terminal sets of  $[B, \dots, I_k]$  (sufficient condition proved before) as well as some other path from the perspective of item  $b$ . However, due to the BBS traversal and Lemma 1, the same item cannot appear in terminal sets of two different paths, and no paths can intersect. This contradicts the assumption. □

**Completeness:** To prove the completeness of  $NAGG_{\mathcal{M}B}$ , we must show that every edge  $i_k.X \rightarrow i_j.Y$  in every ground graph  $GG_{\mathcal{M}\sigma}$ , where  $\sigma \in \Sigma_S$ , has a set of corresponding edges in  $NAGG_{\mathcal{M}B}$ . Let  $\sigma \in \Sigma_{(S)}$  be an arbitrary skeleton and  $i_k.X \rightarrow i_j.Y \in GG_{\mathcal{M}\sigma}$  be an arbitrary edge as a result of dependency  $[I_j, \dots, I_k].X \rightarrow [I_j].Y \in \mathbf{D}$ . The edge yields two sets of relational variables  $\mathbf{P}_k.X = \{P_k.X \mid \exists_{b \in \sigma(B)}, i_k \in P_k|_b\}$  and  $\mathbf{P}_j.Y = \{P_j.Y \mid \exists_{b \in \sigma(B)}, i_j \in P_j|_b\}$ . The construction of  $NAGG_{\mathcal{M}B}$  adds edges corresponding to  $i_k.X \rightarrow i_j.Y \in GG_{\mathcal{M}\sigma}$  as follows:

1. If  $P_k \in \text{extend}(P_j, [I_j, \dots, I_k])$ , then  $P_k.X \rightarrow P_j.Y$  is added according to the definition of  $NAGG_{\mathcal{M}B}$ .
2. If  $P_k \notin \text{extend}(P_j, [I_j, \dots, I_k])$ , but  $\exists_{P'_k} P'_k.X \in \mathbf{P}_k.X \wedge P'_k \in \text{extend}(P_j, [I_j, \dots, I_k])$ , then  $P'_k.X \rightarrow P_j.Y$  is added according to the definition of  $NAGG_{\mathcal{M}B}$ .

*Claim 3.* Above two are only possible conditions for  $NAGG_{\mathcal{M}B}$  i.e.,  $\forall_{P_j|P_j.Y \in \mathbf{P}_j.Y} \exists_{P_k|P_k.X \in \mathbf{P}_k.X} P_k \in \text{extend}(P_j, [I_j, \dots, I_k])$ .

*Proof.* From Proposition 1, we know we can have paths of maximum length four for  $B = E$  and five for  $B = R$ . Moreover, due to the fully connected skeleton with  $N = |\sigma(E)|$  entity instances and  $|\sigma(R)| = \frac{N \times N - 1}{2}$  relationship instances according to Definition 1, the sets  $\mathbf{P}_j.Y$  and  $\mathbf{P}_k.X$  consist all valid paths of the form  $[B, \dots, I_j]$  and  $[B, \dots, I_k]$ , respectively. Thus,  $\text{extend}([B, \dots, I_j], [I_j, \dots, I_k])$  is always a subset of valid paths of the form  $[B, \dots, I_k]$ , and two conditions above are always true.  $\square$

The proof for Corollary 1 is as follows:

*Proof.* The proof follows directly from Theorem 1 that shows  $NAGG_{\mathcal{M}\sigma}$  with extension of relationship existence uncertainty correctly abstracts all ground graphs for the acyclic model  $\mathcal{M}$ . Other extensions of latent and selection attributes are special roles given to the attributes. Thus, Maier (2014)'s Theorem 4.5.3 can be directly applied to  $NAGG_{\mathcal{M}\sigma}$  to prove  $NAGG_{\mathcal{M}\sigma}$  is acyclic.  $\square$

The proof for Theorem 2 follows the proof by Maier (2014) and is provided below:

*Proof.* To establish the soundness of relational d-separation, we must prove that d-separation on a  $NAGG_{\mathcal{M}B}$  implies d-separation on all ground graphs it represents. To show the completeness of relational d-separation, we must prove that d-separation facts that hold across all ground graphs are also entailed by the d-separation on the  $NAGG_{\mathcal{M}B}$ . The introduction of latent and selection attributes only constraint the conditioning set  $\mathbf{Z}$  such that it must always include selection attributes  $\mathbf{S}$  and never include latent attributes  $\mathbf{L}$  for reasoning about d-separation on both ground graphs and  $NAGG_{\mathcal{M}B}$ . The extension for relationship existence uncertainty constraints the relational skeleton and adds implicit dependencies in both ground graphs and  $NAGG_{\mathcal{M}B}$ . Thus, Maier (2014)'s proof of soundness and completeness of relational d-separation applies for  $NAGG$ . Lee and Honavar (2015, 2016) have challenged the completeness of AGG and Maier (2014)'s proof of relational d-separation which is based on completeness of abstraction. But by Theorem 1, we have shown that  $NAGG$  is sound and complete.

**Soundness:** Assume  $\mathbf{X}$  and  $\mathbf{Y}$  are d-separated by  $\mathbf{Z}$  on  $NAGG_{\mathcal{M}B}$ . Assume for contradiction that there exists an item instance  $b \in \sigma(B)$ , for an arbitrary skeleton  $\sigma$ , such that  $\mathbf{X}|_b$  and  $\mathbf{Y}|_b$  are *not* d-separated by  $\mathbf{Z}|_b$  in the ground graph  $GG_{\mathcal{M}\sigma}$ . This implies there must exist a d-connecting path  $p$  from some  $x \in \mathbf{X}|_b$  to some  $y \in \mathbf{Y}|_b$  given all  $z \in \mathbf{Z}|_b$ . Theorem 1 shows that  $NAGG_{\mathcal{M}B}$  is complete suggesting all the edges in the  $GG_{\mathcal{M}\sigma}$  is captured by  $NAGG_{\mathcal{M}B}$ . So, the path  $p$  must be represented by some node in  $\{N_x|x \in N_x|_b\}$  connecting to some node in  $\{N_y|y \in N_y|_b\}$ , where  $N_x$  and  $N_y$  are nodes in  $NAGG_{\mathcal{M}B}$ . If the path  $p$  is d-connected in  $GG_{\mathcal{M}\sigma}$ , then it is also d-connected in  $NAGG_{\mathcal{M}B}$ , implying that  $\mathbf{X}$  and  $\mathbf{Y}$  are *not* d-separated by  $\mathbf{Z}$ . Thus,  $\mathbf{X}|_b$  and  $\mathbf{Y}|_b$  must be d-separated by  $\mathbf{Z}|_b$ .

**Completeness:** Assume  $\mathbf{X}|_b$  and  $\mathbf{Y}|_b$  are d-separated by  $\mathbf{Z}|_b$  in the ground graph  $GG_{\mathcal{M}\sigma}$  for all skeleton  $\sigma$  and for all  $b \in \sigma(B)$ . Assume for contradiction that  $\mathbf{X}$  and  $\mathbf{Y}$  are *not* d-separated by  $\mathbf{Z}$  on  $NAGG_{\mathcal{M}B}$ . This implies there must exist a d-connecting path  $p$  for some relational variable  $X \in \mathbf{X}$  to some  $Y \in \mathbf{Y}$  given all  $Z \in \mathbf{Z}$ . Theorem 1 shows that  $NAGG_{\mathcal{M}B}$  is sound suggesting every edge in  $NAGG_{\mathcal{M}B}$  must correspond to some pair of variables in some ground graph. So, if the path  $p$  is responsible for d-connection in  $NAGG_{\mathcal{M}B}$ , then there must exist some skeleton  $\sigma$  such that  $p$  is d-connecting in  $GG_{\mathcal{M}\sigma}$  for some  $b \in \sigma(B)$ , implying that d-separation does not hold for that ground graph. Thus,  $\mathbf{X}$  and  $\mathbf{Y}$  must be d-separated by  $\mathbf{Z}$  on  $NAGG_{\mathcal{M}B}$ .  $\square$

## A.6 Proofs for identification of individual direct effects

The proof for Lemma 2 first formalizes the Assumption 1 in terms of the Network Structural Causal Model (NSCM), then uses Network Abstract Ground Graph (NAGG) for reasoning about possible adjustment sets that satisfy the backdoor criterion (Pearl 2009) in the presence of selection and latent variables.

*Proof.* The formal implications of Assumption 1 “The network  $G$  and its attributes are measured before treatment assignments and treatments are immutable from assignment to outcome measurement” on the NSCM  $\mathcal{M}(S, \mathbf{D}, \mathbf{f})$  are as follows:

- A. The entity and relationship attributes, i.e.,  $\mathbf{Z}_n \subseteq \mathcal{A}(E)$  and  $\{\text{Exists}, \mathbf{Z}_n\} \subseteq \mathcal{A}(R)$ , are never the descendants of treatment attribute  $X \in \mathcal{A}(E)$  and outcome attribute  $Y \in \mathcal{A}(E)$ . These attributes are commonly referred to as background covariates.

- B. There is no selection bias on treatment and outcome but there could be selection bias on the background covariates, i.e.,  $\mathcal{A}(\mathcal{E}) \cup \mathcal{A}(\mathcal{R}) \setminus \{X, Y\} \in \mathbf{S}$ , where  $\mathbf{S}$  indicates a set of attributes marked as selected. Note that the absence of selection bias is the stronger assumption and the experimental or observational studies for causal inference studies typically select certain populations of interest based on the background covariates. For the selected population, there is no further selection based on treatment and outcome is a reasonable assumption for experimental or prospective observational data.
- C. Although all attributes could be auto-regressive (e.g.,  $[E].Y^L \rightarrow [E].Y$ ) or contagious (e.g.,  $[E, R, E].Y^L \rightarrow [E].Y$ ), the treatment is assumed to be immutable during the study period. This implies the time-lagged treatment attributes do not directly affect the outcome, i.e.,  $\{[E].X^L \rightarrow [E].Y, [E, R, E].X^L \rightarrow [E].Y\} \notin \mathbf{D}$ . All time-lagged attributes  $\{X^L, Y^L, \mathbf{Z}_n^L, \mathbf{Z}_e^L, \text{Exists}^L\} \subseteq \mathbf{L}$ , where  $\mathbf{L}$  is a set of attributes marked as latent.

For node attributes  $\mathbf{Z}_n$  and edge attributes  $\mathbf{Z}_e$ , we denote relational variables  $[E].\mathbf{Z}_n, [E, R].\mathbf{Z}_e, [E, R, E].\mathbf{Z}_n$ , and  $[E, R, E, R].\mathbf{Z}_e$  with the notations  $Z_i \in \mathbb{R}^d, Z_r \in \mathbb{R}^{N' \times d'}, Z_{-i} \in \mathbb{R}^{N' \times d}$ , and  $Z_{-r} \in \mathbb{R}^{N' \times N'-1 \times d'}$ , respectively, where  $N' = |\mathcal{V}| - 1$  and  $< d, d' >$  are constants. Let  $E_r \in \{0, 1\}^{N' \times 1}$  and  $E_{-r} \in \{0, 1\}^{N' \times N'-1 \times 1}$  be the relationship existence indicator variables  $[E, R].\text{Exists}$  and  $[E, R, E, R].\text{Exists}$ , respectively. Let  $\mathbf{L}_v$  and  $\mathbf{S}_v$  denote sets of latent and selection variables, respectively.

Since our causal estimand of individual direct effects (IDE), has peer treatments as a conditional in Equation 2, the identification should consider  $X_{-i}$ , i.e.,  $[E, R, E].X$  as observed and we need to find an adjustment set  $\{X_{-i}, \mathcal{Z}_i\}$ . To prove Lemma 2, we have to show that if there exists any valid adjustment set  $\mathbf{W}$ , where  $X_{-i} \in \mathbf{W} \wedge \mathbf{W} \cap \mathbf{L}_v = \emptyset \wedge \mathbf{W} \cap \mathbf{S}_v = \mathbf{S}_v$ , then the set  $X_{-i}, \mathcal{Z}_i, \mathbf{S}_v$ , where  $\mathcal{Z}_i = \{Z_i, Z_r, Z_{-i}, Z_{-r}, E_r, E_{-r}\}$  is also a valid adjustment set. The restrictions in  $\mathbf{W}$  follow from the implications of latent and selection variables in the adjustment set.

Although the unconfoundedness condition, i.e.,  $\{Y_i(X_i = 1), Y_i(X_i = 0)\} \perp\!\!\!\perp X_i | \mathbf{W}$ , is untestable, causal reasoning of d-separation between  $X_i$  and  $Y_i$  can be used in the ‘‘mutilated’’ SCM ( $\mathcal{G}_{\bar{X}_i}$ ) where outgoing edges from treatment  $X_i$  are removed (Pearl 2009; Bareinboim and Pearl 2016).

There can be arbitrary dependencies between all possible background variables and these variables may or may not affect treatment and outcome.

Proof by contradiction. Let  $\mathbf{W}$  satisfy the unconfoundedness condition, i.e.,  $\mathbf{W}$  d-separates  $X_i$  and  $Y_i$  in  $\mathcal{G}_{\bar{X}_i}$ , but the set  $\{X_{-i}, Z_i, Z_r, Z_{-i}, Z_{-r}, E_r, E_{-r}\}$  does not for contradiction.

**Case I:** *There is latent confounding between  $X_i$  and  $Y_i$ , i.e.,  $X_i \leftrightarrow Y_i$ .*

This contradicts the condition that  $\mathbf{W}$  d-separates  $X_i$  and  $Y_i$  in  $\mathcal{G}_{\bar{X}_i}$  because there exists an open path due to unobserved confounding.

**Case II:** *There exist paths  $X_i \leftrightarrow C$  and  $D \leftrightarrow Y_i$  for any colliders  $C$  and  $D$  such that  $\{C, D\} \notin \{X_i, Y_i, Y_{-i}\}$ , where  $C = D$  or there exist open path from  $C$  to  $D$  (e.g., collider chaining), with a latent common cause between  $C$  and the treatment  $X_i$  and a separate latent common cause between  $D$  and the outcome  $Y_i$ .*

In this case, if collider  $C$  is peer treatments, i.e.,  $X_{-i}$ , then it must be observed for estimating Equation 2. The conditioning opens a path from  $X_i$  to  $Y_i$  via the collider. If the collider is any background covariate then, the selection of the background covariates opens the path  $X_i$  to  $Y_i$  via the collider. Any open paths from  $C$  and  $D$  for  $C \neq D$  follows the same reasoning. These cases contradict the condition that  $\mathbf{W}$  d-separates  $X_i$  and  $Y_i$  in  $\mathcal{G}_{\bar{X}_i}$ .

**Case III:** *There exist a path  $X_i \leftarrow L_v \rightarrow Y_{-i}$ , where  $L_v \in \{L_i, L_r, L_{-i}, L_{-r}\}$ .*

In this case, although we have  $X_i \leftrightarrow Y_{-i} \leftrightarrow Y_i$ ,  $Y_{-i}$  is not observed and does not belong to the selection set and cannot directly open paths like case II. However,  $X_i \leftrightarrow Y_{-i}$  suggests a dependency  $L_v \rightarrow Y_{-i}$ , where  $L \in \mathbf{L}$  be a latent node or edge attribute and  $L_v$  the corresponding variable. NSCM specifies dependencies in the canonical form. Therefore, for this extended dependency  $L_v \rightarrow Y_{-i}$  (purple arrows in Figure 11), there must be some explicit dependency that needs to be considered for the identifiability of causal effects. Figure 11 illustrates equivalence for  $L_v \in \{L_i, L_r, L_{-i}, L_{-r}\}$  to cases II, I, II, and I respectively. The purple arrow shows  $L_v \rightarrow Y_{-i}$  dependency while the black arrow shows  $L_v \rightarrow X_i$  dependency. These dependencies are extended and shown as dotted edges. For this case the condition that  $\mathbf{W}$  d-separates  $X_i$  and  $Y_i$  in  $\mathcal{G}_{\bar{X}_i}$  does not hold.

For all other cases, from Proposition 1, we have a maximum of four paths for entity perspective. The adjustment set  $\{X_{-i}, Z_i, Z_r, Z_{-i}, Z_{-r}, E_r, E_{-r}\}$  covers all observed variables except  $Y_{-i}$ . Adjusting on  $Y_{-i}$  can open the colliders. Thus,  $\{X_{-i}, Z_i, Z_r, Z_{-i}, Z_{-r}, E_r, E_{-r}\}$  is the maximal adjacency set that does not open any more colliders and block all the mediated backdoor paths if first three cases do not exist. This contradicts the set  $\{X_{-i}, Z_i, Z_r, Z_{-i}, Z_{-r}, E_r, E_{-r}\}$  does not satisfy unconfoundedness when a set  $\mathbf{W}$  does. □

**Discussion.** The implication of Lemma 2 is that under Assumption 1, the underlying data generation of treatment and outcome can be described by functions  $f_X$  and  $f_Y$  in our general NSCM as:

$$X_i = f_X(Z_i, Z_r, Z_{-i}, Z_{-r}, E_r, E_{-r}, X_i^L, X_{-i}^L, \epsilon_X) \text{ and} \quad (4)$$

$$Y_i = f_Y(X_i, X_{-i}, Z_i, Z_r, Z_{-i}, Z_{-r}, E_r, E_{-r}, Y_i^L, Y_{-i}^L, \epsilon_Y), \quad (5)$$

where  $\{X_i^L, X_{-i}^L, Y_i^L, Y_{-i}^L\}$  are latent time-lagged variables for treatment and outcome. The NSCM allows modeling latent homophily, contagious treatments or outcomes, and selection bias. Although all relational variables may not affect the treatment/outcome, the above NSCM does not change the identifiability of causal effects. Considering the maximal adjacency set is helpful to close the path between separate colliders  $C$  and  $D$  for case II as well as the backdoor paths (Pearl 2009) mediated by

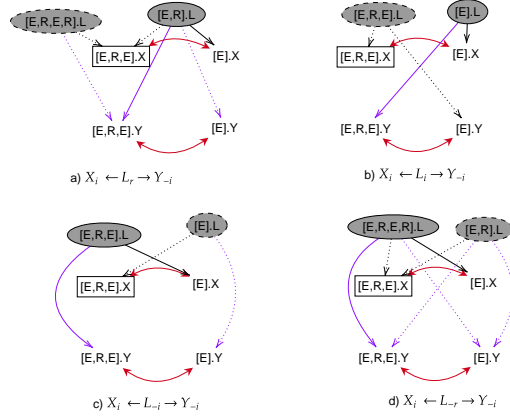


Figure 11: Illustration of contradiction of condition **W** d-separates  $X_i$  and  $Y_i$  in  $\mathcal{G}_{X_i}$  that for Case III: *There exist a path  $X_i \leftarrow L_v \rightarrow Y_{-i}$ , where  $L_v \in \{L_i, L_r, L_{-i}, L_{-r}\}$ .* Depending on the path of the latent variable in Case III, other dependencies derived (dotted) from NSCM/NAGG show equivalence with Case I and Case II.

the maximal set. Also, having a maximal adjustment set helps to capture underlying influence mechanisms and effect modifications. We have identified conditions under which observational data is not sufficient to guarantee the identifiability of causal effects. Further assumptions or experiments are required in such cases.

The proof of Corollary 2 applies do-calculus for experimental data with incoming edges to unit treatment and peer treatments removed but allowing correlation between treatments. For observational data, we use Lemma 2’s condition, i.e., the unconfoundedness assumption.

*Proof. Case 1: Experimental data.* In this case, the treatments are assigned to units randomly or according to some experimental design. Therefore, the treatments  $\langle X_i, X_{-i} \rangle$  are exogenous and do not depend on observed contexts  $\mathcal{Z}_{-i}$  or unobserved confounders. The treatment assignments, however, can be correlated depending on the experimental design. Figure 12 depicts the causal graph for the experimental data with exogenous but correlated treatments (green bi-directed edge). Although the relational variables  $\{Z_i, Z_r, Z_{-i}, Z_{-r}, E_r, E_{-r}\}$  can have arbitrary causal dependence among themselves, we represent these variables with a single node in the causal graph for simplicity. The black edges in the causal diagram show dependencies between treatment, outcome, and context variables. The blue edges show the dependencies due to contagion where a unit’s outcome, measured some time steps after treatment assignment, may be influenced by peers’ past outcomes. The dashed blue bi-directed edge indicates the time-lagged outcomes may be correlated due to contagion in earlier time steps. Figure 12 depicts treatment  $X_i$  in the blue circle, outcome  $Y_i$  in the red circle, conditional variables  $\mathcal{Z}_i$  and  $X_{-i}$  in rectangles, and latent variables in the shaded circle.

The counterfactual  $E[Y_i(X_i = \pi_i)|X_{-i}, \mathcal{Z}_i]$  can be written in terms of do-expression as  $E[Y_i|do(X_i = \pi_i), X_{-i}, \mathcal{Z}_i]$  because both  $\{X_{-i}, \mathcal{Z}_i\}$  are non-descendants of  $X_i$  (Pearl 2009). Then,  $E[Y_i|do(X_i = \pi_i), X_{-i}, \mathcal{Z}_i]$  can be estimated with  $E[Y_i|X_i = \pi_i, X_{-i}, \mathcal{Z}_i]$  in the experimental data because  $\{X_{-i}, \mathcal{Z}_i\}$  satisfies backdoor criterion (Pearl 2009) from  $X_i$  to  $Y_i$ . In the causal graph with edges outgoing from treatment  $X_i$  removed, the conditional set  $\{X_{-i}, \mathcal{Z}_i\}$  d-separates  $X_i$  and  $Y_i$  and satisfies Pearl’s second rule of do-calculus (Bareinboim and Pearl 2016), enabling the substitution.

**Case 2: Observational data.** For the identification of causal effects from observational data, we have an additional assumption of unconfoundedness, i.e.,  $\{Y_i(X_i = 1), Y_i(X_i = 0)\} \perp\!\!\!\perp X_i|X_{-i}, \mathcal{Z}_i$  (Lemma 2). The counterfactual  $E[Y_i(X_i = \pi_i)|X_{-i}, \mathcal{Z}_i]$  can be written in terms of do-expression as  $E[Y_i|do(X_i = \pi_i), X_{-i}, \mathcal{Z}_i]$  because both  $\{X_{-i}, \mathcal{Z}_i\}$  are non-descendants of  $X_i$  (Pearl 2009). The term  $E[Y_i|do(X_i = \pi_i), X_{-i}, \mathcal{Z}_i]$  can be replaced by conditional  $E[Y_i|X_i = \pi_i, X_{-i}, \mathcal{Z}_i]$  using Pearl’s second rule of do-calculus (Bareinboim and Pearl 2016) if  $\{X_{-i}, \mathcal{Z}_i\}$  d-separates  $X_i$  and  $Y_i$  in the mutilated graph with outgoing edges from  $X_i$  removed. Assume, for contradiction, this d-separation does not exist. However, this contradicts the unconfoundedness assumption where  $X_i$  is independent of counterfactual outcomes  $\langle Y_i(1), Y_i(0) \rangle$  given  $\{X_{-i}, \mathcal{Z}_i\}$ . Therefore, the counterfactual  $E[Y_i(X_i = \pi_i)|X_{-i}, \mathcal{Z}_i]$  can be estimated with  $E[Y_i|X_i = \pi_i, X_{-i}, \mathcal{Z}_i]$  under unconfoundedness assumption.  $\square$

## A.7 Estimators and hyperparameters

We start with the description of hyperparameters of the proposed IDE-TARNet estimator. Then, we discuss hyperparameters for baselines in each experimental setting. Finally, we describe the computational resources used for the experiments.

We separate IDE-TARNet into two components: individual direct effects (IDE) encoder to learn feature and exposure mapping and TARNet for counterfactual prediction. Since our feature and exposure embeddings try to capture all potential heterogeneity contexts, most of these contexts could be irrelevant for underlying data generation. So, we include a Batch Normalization layer with *tanh* activation function after the first *MLP* layer in the TARNet module. The Batch Normalization layer adds regularization to mitigate the effect of irrelevant features.

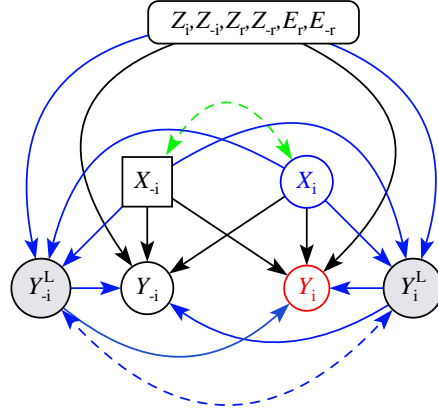


Figure 12: Causal diagram for experimental data ( $G^{exp}$ ).

The fundamental challenge with causal effect estimation tasks is that we do not have ground truth for any causal effects to tune hyperparameters and the models have to rely on generalizing for the observed factual outcomes. The regularization to avoid over/underfitting relies on smoothing the variance in estimated causal effects. This is particularly important for our causal inference under heterogeneous peer influence (HPI) task to maintain invariance to non-relevant contexts while retaining expressiveness. Also, we train our models starting with a higher learning rate and gradually decreasing the learning rates.

#### Hyperparameters for IDE-TARNet estimator.

- `maxiter`: Maximum number of epochs to train (default 300)
- `val`: Fraction of nodes to be used in validation set for model selection or early stopping (default 0.2)
- `lr`: Learning rate for the encoder, i.e., feature and exposure embeddings, (default 0.02)
- `lrest`: Learning rate for the estimator, i.e., counterfactual predictors, (default 0.2)
- `lrstep`: Change learning rate after 1 epochs (default 50)
- `lrgamma`: Decay learning rate by multiplying it with this value (default 0.5)
- `clip`: Clip gradient values of estimator (default 3)
- `max_patience`: Early stopping if validation loss (without regularization) does not improve for given epochs (default 300, i.e., no early stopping)
- `weight_decay`: L2 regularization parameter for the Adam optimizer (default  $1e - 5$ )
- `fdim`: Dimension of hidden units for node and peer features (default 32 for synthetic and 64 for semi-synthetic data)
- `edim`: Dimension of hidden units for edge features (default 4)
- `inlayers`: MLP layers for the encoder (default 2). We chose 2 layers to capture non-linear feature mapping before summarization with GCN.
- `dropout`: Dropout probability (default 0). We rely on L2 regularization, batch normalization, and smoothing regularization and do not use dropout.
- `normY`: Whether outcome should be normalized for training (default False)
- `alpha`: Parameter for representation balancing regularization (Shalit, Johansson, and Sontag 2017; Guo, Li, and Liu 2020) (default 0 for TARNet and 0.5 for CFR). Although IDE-TARNet could be converted to IDE-CFR by passing any alpha except 0, we do not report experiments for this estimator because it has additional computation cost and hyperparameter selection. We substitute the regularization obtained by representation balancing with cheaper smoothing regularization explained next.
- `reg`: Whether smoothing regularization should be enabled (default True). If set to true, we fix decay parameter  $\gamma = 3$  and select the model with the best validation loss (without regularization) between two settings of scaling parameter  $\lambda_s = 0.1$  and  $\lambda_s = 1.0$ . The regularization is only enabled after 150, i.e., 50%, epochs to estimate the variance of predicted causal effects and decide the strength of smoothing. Without smoothing, the performance of IDE-TARNet is slightly worse, when the underlying causal effects are uniform.

**Hyperparameters for baselines.** We compare the performance of our method with the NetEst (Jiang and Sun 2022) estimator and baselines (Network Deconfounder (ND) (Guo, Li, and Liu 2020), ND-INT, GCN-TARNet, GCN-TARNet-INT, MLP-CFR, and MLP-CFR-INT) implemented in the NetEst paper<sup>1</sup>. NetEst (Jiang and Sun 2022) focuses on estimating "insulated" individual effects, peer effects, and overall effects for within-sample data (i.e., data available for training the model) as well as out-of-sample data (i.e., data unavailable for training the model). NetEst uses regularization by making features less predictive of treatment assignments and homogenous peer exposure. We adapt NetEst to estimate individual effects instead of "insulated" individual effects but find the performance very poor. This may be because NetEst concatenates features, peer exposure, and treatment before counterfactual prediction, and it is not agnostic to treatment like TARNet and CFR architectures (Shalit, Johansson, and Sontag 2017). The value of treatment may be lost in our settings where individual effects have a small coefficient and peer exposure has a large coefficient. Although we focus on individual direct effect estimation for within-sample data, we use NetEst with "insulated" individual effects as a baseline for two experiment settings because "insulated" individual effects are equivalent to individual effects without interaction with peer exposure.

We use all default hyperparameters of NetEst except we set the epochs to train the treatment predictor and peer exposure predictor to 1 instead of 50 to save computation time. Interestingly, we find the performance of NetEst with parameters  $dstep = 1$  and  $d_zstep = 1$  is better than the default settings and report these performances in Figures 5-8. For the BART baseline, we use python-based implementation<sup>2</sup> and use the default parameters. BART is popular for good performances without hyperparameters tuning (Hill 2011). For other baselines, we use default parameters but adapt them to estimate individual direct effects instead of "insulated" individual effects. For the ablation study in Figure 9, the baselines use our TARNet/CFR module and similar hyperparameters to that of the IDE-TARNet estimator. For the ablation study, we follow Yuan, Altenburger, and Kooti (2021)'s implementation<sup>3</sup> to generate data for structural diversity as a peer influence mechanism and to extract causal motifs.

**Computational resources.** All the experiments are performed in a machine with the following resources.

- CPU: AMD EPYC 7662 64-Core Processor (128 CPUs)
- Memory: 256 GB RAM
- Operating system: Ubuntu 20.04.4 LTS
- GPU: NVIDIA RTX A5000 (24 GB)
- CUDA Version: 11.4

---

<sup>1</sup><https://github.com/songjiang0909/Causal-Inference-on-Networked-Data>

<sup>2</sup><https://github.com/JakeColtman/bartpy>

<sup>3</sup><https://github.com/facebookresearch/CausalMotifs>